

Synthesis and photochemical studies of 2-nitrobenzyl-caged *N*-hydroxysulfonamides

Yang Zhou^a, Vinay Bharadwaj^{b,c}, Mohammad S. Rahman^a, Paul Sampson^a, Nicola E. Brasch^{b,c,**}, Alexander J. Seed^{a,*}

^a Department of Chemistry and Biochemistry, Kent State University, Kent, OH 44242, USA

^b School of Science, Auckland University of Technology, Auckland 1142, New Zealand

^c Dodd-Walls Centre for Quantum and Photonic Technologies, New Zealand

ABSTRACT

Recently, *N*-hydroxysulfonamides (RSO₂NHOH) caged by photolabile protecting groups have attracted significant interest as potential photoactive nitroxyl (HNO) donors. The selectivity of the desired HNO generation pathway from photocaged *N*-hydroxysulfonamides versus a competing pathway involving O-N bond cleavage is dependent on the specific photodeprotection mechanism of the phototrigger. We present a new class of photocaged *N*-hydroxysulfonamides incorporating the well-established *o*-nitrobenzyl photoprotecting group, including a derivative incorporating an additional carbonate linker. Photodecomposition of *o*-NO₂Bn-ON(H)SO₂CF₃ and the corresponding 2-nitro-4,5-dimethoxybenzyl analog generated the desired HNO and CF₃SO₂⁻ as a minor pathway, with competing photoinduced O-N bond cleavage to release CF₃SO₂NH₂ as the major photodecomposition pathway. Photolysis of the corresponding -SO₂CH₃ analogs resulted in O-N bond cleavage only. The presence of the *o*-nitro substituent was shown to be essential for photoactivity. Photorelease of the parent HNO donor CH₃SO₂NHOH was observed as the major product upon irradiation of *o*-NO₂Bn-OC(O)ON(H)SO₂CH₃, with the desired HNO release and O-N bond cleavage occurring as minor pathways. Photoproduct quantum yields for each species have been determined by actinometry. The effect of solvent, pH and air on the mechanism of photodecomposition was studied for *o*-NO₂Bn-ON(H)SO₂CH₃. The ratio of the solvents in the solvent mixture (CH₃CN and phosphate buffer, pH 7.0), the pH of the aqueous component of the buffer, and the presence of oxygen did not affect the amount of each photoproduct and the observed rate constant for O-N bond cleavage. Possible mechanisms for the various pathways are proposed.

1. Introduction

The importance of nitroxyl (HNO) is increasingly recognized in biochemical and biological systems [1–2], due to its significant promise in therapeutic and pharmaceutical applications [3–9]. Recent clinical trials on the HNO prodrug CXL-1020 and the second generation analog Cimlanod (BMS-986231 or CXL-1427) highlight the potential of HNO in the treatment of congestive heart failure *via* the improvement of Ca²⁺ handling and myofilament Ca²⁺ sensitivity [7–9]. Compared to the widely studied nitric oxide (NO) [10], the biological roles of HNO are less well understood to date. HNO reactivity studies are more challenging due to its rapid dimerization ($k = 8 \times 10^6 \text{ M}^{-1} \text{ s}^{-1}$) and subsequent decomposition to nitrous oxide and water [11]. Therefore, HNO precursors (typically called HNO donors) which decompose to release HNO are required for studies of the chemical and biochemical reactivity of this important molecule [12–15].

The rate of generation of HNO is dependent on the decomposition chemistry of each HNO donor. Angeli's salt (AS) and Piloty's acid (PA) are the most commonly used HNO donors [13–15], Fig. 1. Several other

classes of HNO donors have also been reported, including PA-based derivatives [16–18], *N*/*O*-substituted hydroxylamines [19–24], primary amine-based diazeniumdiolates [25–27], acyloxy nitroso compounds [28–31], precursors of acyl nitroso species [32–39], and metal nitrosyls [40–43]. Most of these HNO donors liberate HNO upon protonation [19,41,43], deprotonation [16–17, 44], and/or hydrolysis in solution [20,28]. A limited number of photochemical approaches for HNO generation have also been reported, including retro-cycloaddition reactions [34–36, 38–39], the combination of an HNO donor with a pH photoactuator [45], and the use of caged *N*-hydroxysulfonamides using a photocaging group (PCG) [46–49]. Most of these photomediated approaches reported to date have drawbacks, including low HNO generation with competition from thermal or photochemical side reactions leading to the generation of NO in addition to HNO, and/or other side products.

Our group developed a new family of photoactivatable *N*-alkoxysulfonamide HNO donors caged by the *O*-(3-hydroxy-2-naphthalenyl) methyl photolabile protecting group [46–47], Fig. 2. Competition between concerted C-O/N-S bond cleavage to release HNO and undesired

* Corresponding author at: Department of Chemistry and Biochemistry, Kent State University, Kent, OH 44242, USA

** Corresponding author at: School of Science, Auckland University of Technology, Auckland 1142, New Zealand.

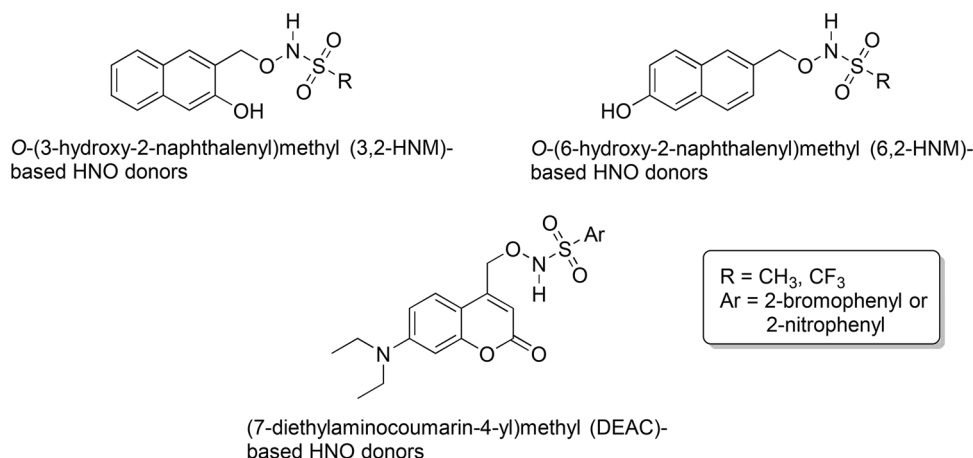
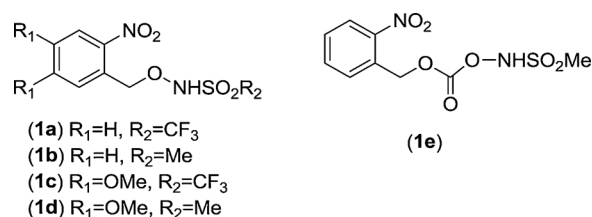
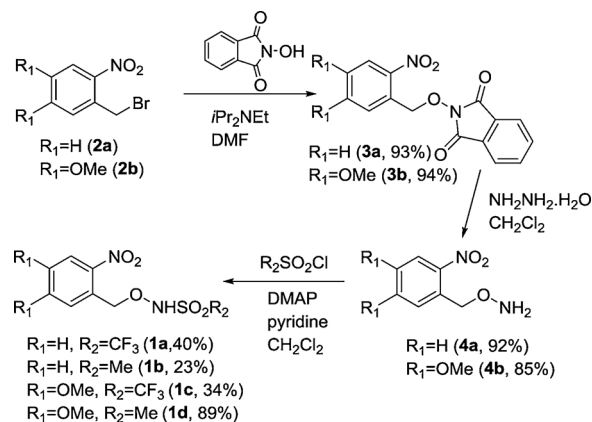
E-mail addresses: nbrasch@aut.ac.nz (N.E. Brasch), aseed@kent.edu (A.J. Seed).



Fig. 1. Structures of Angeli's salt and Piloty's acid.

O-N bond cleavage was found to be strongly solvent dependent [47]. In addition, the nature of the sulfinate leaving group played a major factor in determining the selectivity for HNO generation versus O-N bond cleavage. Very recently, we extended these studies to the isomeric O-(6-hydroxy-2-naphthalenyl)methyl congeners (Fig. 2), where significantly enhanced selectivity for HNO release was observed [49]. Nakagawa et al. recently reported (7-diethylaminocoumarin-4-yl)methyl-caged PA derivatives (Fig. 2; Ar = 2-bromophenyl and 2-nitrophenyl) as visible-light activated HNO generators [48]. However, < 10% HNO was released due to competition from a competing reaction resulting in an oxime product.

Chromophores incorporating the 2-nitrobenzyl moiety are among the most widely used PCGs [50–56]. Their photocaging mechanisms have been studied in detail [57], and the 2-nitrobenzyl (NB) PCG and the closely related 4,5-dimethoxy-2-nitrobenzyl (MeONB) PCG have been widely utilized to cage a range of biologically important molecules [50, 58–74]. In particular, the NB phototrigger has been successfully used to photocage hydroxylamine derivatives. For example, McCulla et al. reported that 2-nitrobenzyl benzohydroxamate yields benzohydroxamic acid (75%) upon irradiation [75]. These authors explain the high selectivity for the desired C-O bond cleavage seen in their system by pointing out that (i) arenosulfonylhydroxamates can afford photolysis products derived from S–N bond homolysis but that this typically occurs only after extended irradiation, and (ii) competing N-O bond homolysis requires higher energy irradiation wavelengths than needed for photoactivation of the NB group. Photocaged suberoylanilide hydroxamic acid and its derivatives can also be released using the MeONB phototrigger [76–77]. Various hydroxylamine intermediates are photochemically generated (maximum 95%) from caged analogs by use of the NB phototrigger [78]. McCune et al. successfully obtained several hydroxylamino acid compounds *via* photocaging of the NB group [79]. Recently, Qvortrup et al. reported photolytic release of hydroxamic acids caged by the NB PCG in protic solvents in high yield [80–81], while carboxamides were instead obtained in aprotic solvent from competing N-O bond cleavage [81]. Finally, carbonate and carbamate linkers between the NB/MeONB group and a caged substrate have also been widely used for photoprotection of molecules of interest [63,82]. Interestingly, the entire photocaging process in such systems was reported to occur within 32 μ s under irradiation at 350 nm [63].

Fig. 2. Structures of the *N*-alkoxysulfonamide donors containing 3,2-HNM, 6,2-HNM and DEAC PCGs.Fig. 3. Structures of the NB- and MeONB-photocaged *N*-hydroxysulfonamides synthesized in this study.

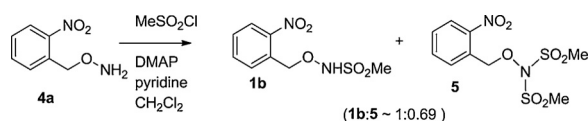
Scheme 1. Synthetic pathway for the preparation of targets 1a-1d.

Given the numerous examples of successful photocaging using the NB and MeONB PCGs, it was of interest to explore the potential of *N*-hydroxysulfonamides caged with a NB or a MeONB group in the absence and presence of the additional carbonate linker for photochemical HNO generation. In this work, we describe the synthesis and photochemistry of compounds 1a-1e, Fig. 3.

2. Results and Discussion

2.1. Synthesis and Characterization of NB- and MeONB-protected *N*-hydroxysulfonamides 1a-1e

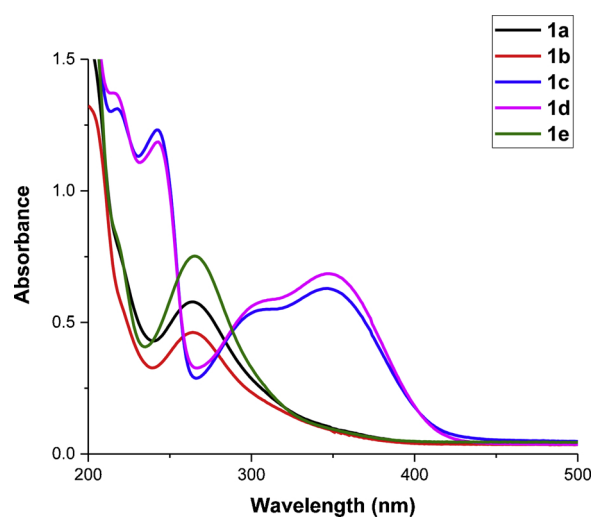
Targets 1a-1d were synthesized according to the approach outlined in Scheme 1. Alkyl bromides 2a and 2b were subjected to an S_N2 reaction with *N*-hydroxyphthalimide to yield hydroxylamine adducts 3a and 3b. Deprotection to free amines 4a and 4b was accomplished using hydrazine monohydrate. This was followed by an *N*-trifluoromethanesulfonylation or *N*-methanesulfonylation to afford targets

Fig. 4. Methanesulfonylation of free amine **4a**.

1a-1d. During the methanesulfonylation of **4a**, in addition to the desired target **1b**, a bis-methanesulfonylation product **5** was also obtained (see Fig. 4). The ratio of **1b**:**5** was $\sim 1:0.69$ based on the analysis of the crude ^1H NMR spectrum; however, these products were readily separated.

Target **1e** was synthesized in three steps as shown in Scheme 2. *o*-Nitrobenzyl alcohol (**6**) was reacted with triphosgene (**7**) to generate the chloroformate intermediate, which was directly treated with *N*-BOC-protected hydroxylamine (**8**) to yield carbonate **9**. *N*-Sulfonylation of **9** by methanesulfonyl chloride gave intermediate **10**. This compound was found to be unstable during both untreated and base-treated silica chromatography. Therefore, it was directly utilized in the next step without purification. Removal of the BOC protecting group from **10** was achieved upon treatment with trifluoroacetic acid (TFA) to afford **1e** in 85% yield over two steps.

We also attempted to prepare the analogous carbonate-linked trifluoromethanesulfonamide (see Scheme 3). *N*-Trifluoromethanesulfonylation of **9** proved unsuccessful under various conditions (Pathway 1; see Table S1 in Supporting Information). Moreover, the synthesis of target **1f** via a modified one-pot *N*-deprotection/*N*-trifluoromethanesulfonylation sequence also failed (pathway 2). After continuous stirring and monitoring for 4 days, no sign of

Fig. 5. UV-Vis spectra of **1a-1e** (1.50×10^{-4} M) in a mixture of water and MeCN (92:8, v/v) at 25 °C.

product **1f** was observed based on crude ^1H and ^{19}F NMR analysis. 2-Nitrobenzyl alcohol **6** was instead obtained as the primary decomposition product.

UV-Vis spectra for compounds **1a-1e** are shown in Fig. 5. The molar extinction coefficients for targets **1a-1e** were determined (Fig. S1-S5) and are summarized in Table 1. The UV-vis spectra of **1c** and **1d** are shifted to lower energies compared with **1a-b** and **1e**, due to the

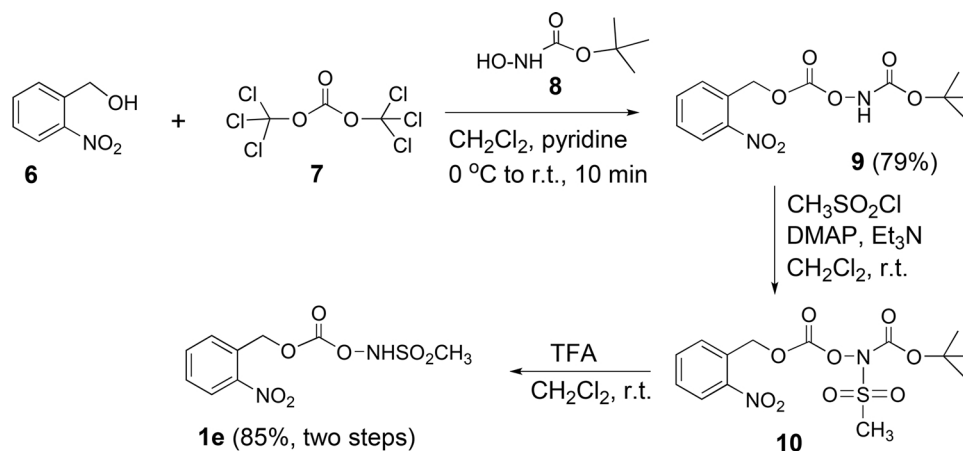
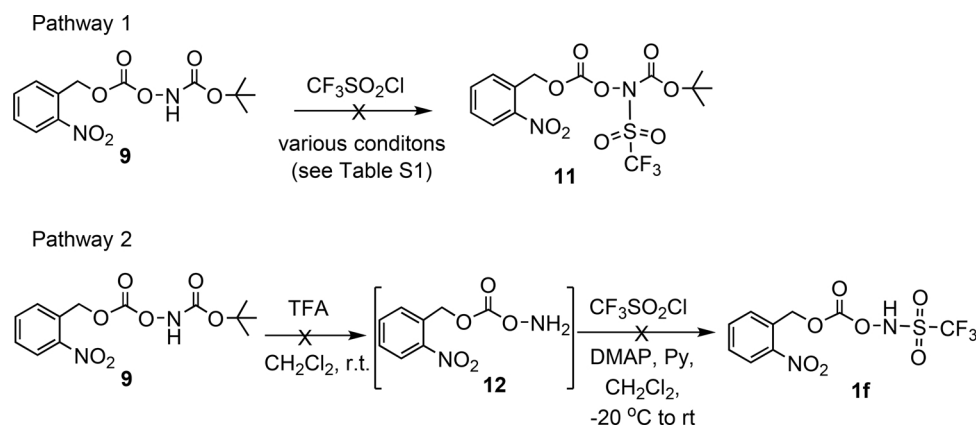
Scheme 2. Synthetic pathway for the preparation of target **1e**.Scheme 3. Unsuccessful synthetic approaches to **1f**.

Table 1

Molar extinction coefficients for compounds **1a-1e** in a mixture of water and MeCN (92:8, v/v; 25.0 °C)

Compound	Molar extinction coefficients ($M^{-1} \text{ cm}^{-1}$)
1a	$(3.68 \pm 0.02) \times 10^3$ (264 nm)
1b	$(2.95 \pm 0.02) \times 10^3$ (264 nm)
1c	$(3.99 \pm 0.02) \times 10^3$ (351 nm)
1d	$(4.44 \pm 0.04) \times 10^3$ (351 nm)
1e	$(4.86 \pm 0.03) \times 10^3$ (264 nm)

presence of the electron-donating methoxy substituents on the phenyl ring.

2.2. Characterization of the photoproducts obtained by steady state irradiation of HNO donors 1a-1e

The photoproducts of **1a-1e** were determined, by steady state irradiation in an anaerobic mixture of phosphate buffer (0.10 mM, pH 7.00) and CD_3CN (40:60, v/v) using a Rayonet photoreactor (RMR-600, 300 nm lamps, 4 W). All compounds **1a-1e** were stable in this solvent mixture in the dark for at least 12 h (NMR spectroscopy). Anaerobic conditions were initially used, to ensure that potential side reactions involving oxygen did not occur. Irradiation centered at 300 nm should allow for selective excitation of the nitro group in the NB chromophore [81], which we anticipated, by analogy with the work of McCulla [75] and Qvortrup [55,80–81], would lead to selective C-O bond cleavage in protic media.

Fig. 6a shows ^{19}F NMR spectroscopy data obtained during the photolysis of **1a**. $\text{CF}_3\text{SO}_2\text{NH}_2$ was formed as the major product (-80.3 ppm, 91%), while CF_3SO_2^- was observed as a minor byproduct (-87.9 ppm, 9%). The photodecomposition was complete after ~

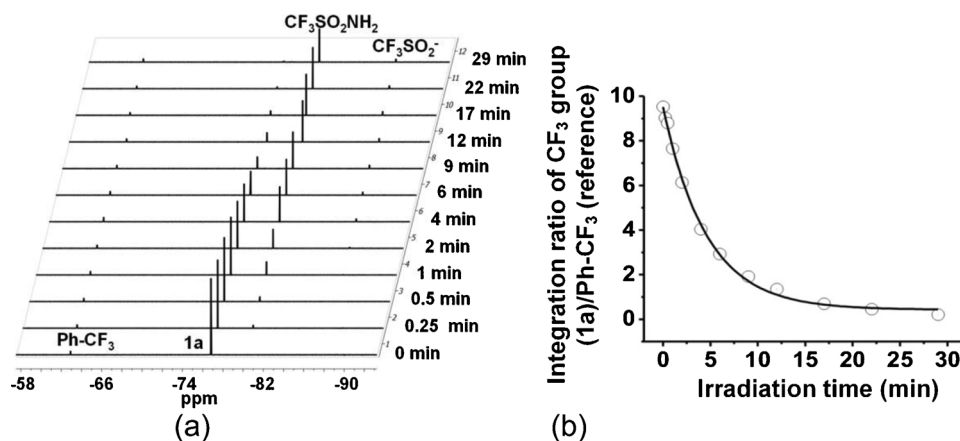
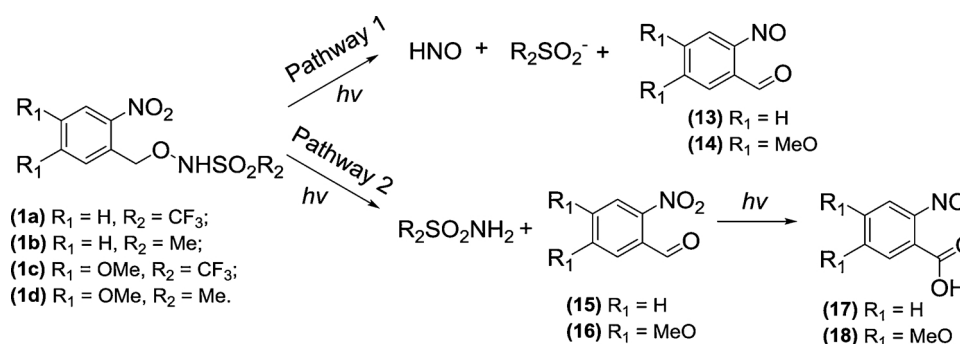


Fig. 6. (a) ^{19}F NMR spectra for the photodecomposition of **1a** (3.89 mM) in a mixture of phosphate buffer (0.10 mM, pH 7.00) and CD_3CN (40:60, v/v). (b) Best fit of the peak area of **1a** (CF_3 group) versus time to a first-order rate equation, giving $k_{\text{obs}} = 0.22 \pm 0.01 \text{ min}^{-1}$ ($t_{1/2} \sim 3.2 \text{ min}$).



Scheme 4. Photolytic pathways observed from **1a-1d** (Pathway 1: C-O bond cleavage; Pathway 2: O-N bond cleavage).

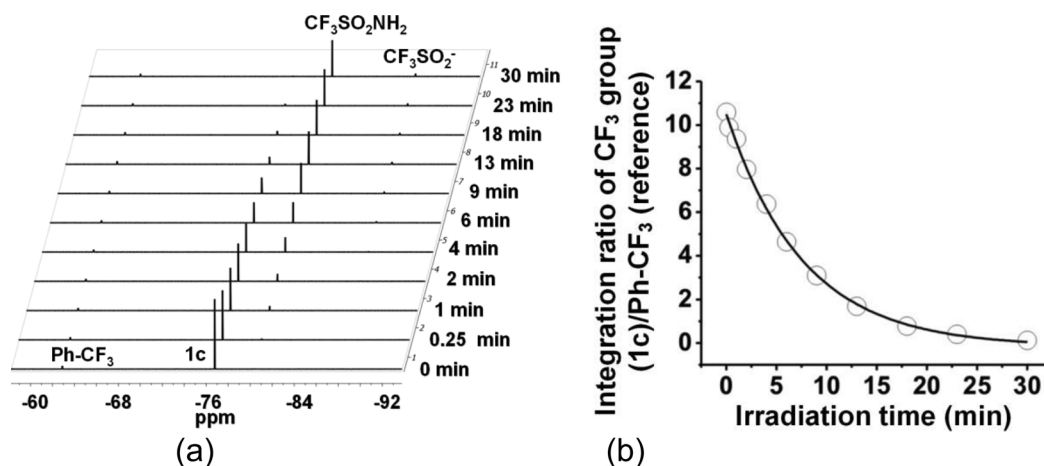


Fig. 7. (a) ^{19}F NMR spectra for the photodecomposition of **1c** (3.89 mM) in a mixture of phosphate buffer (0.10 mM, pH 7.00) and CD_3CN (40:60, v/v). (b) Best fit of the peak area of **1c** (CF_3 group) versus time to a first-order rate equation, giving $k_{\text{obs}} = 0.13 \pm 0.01 \text{ min}^{-1}$ ($t_{1/2} \sim 5.3 \text{ min}$).

reduce both nitro and nitroso compounds [83–84]. A control experiment revealed that **1a** did not react with triphenylphosphine in the absence of light. Thus, we speculate that a photoredox reaction between nitroso compound **17** and triphenylphosphine may be occurring that would potentially lead to azoxybenzene and phosphine oxide products (^1H NMR analysis of the products was inconclusive due to overlapping of complex aromatic signals). This result would be consistent with previously reported chemistry by Cadogan et al. [83–84].

The photodecomposition of **1c** was studied by ^{19}F NMR spectroscopy under the same solvent conditions. After $\sim 30 \text{ min}$ irradiation, $\text{CF}_3\text{SO}_2\text{NH}_2$ was obtained as the major ^{19}F -containing product ($\sim 93\%$), with only 7% CF_3SO_2^- generated, Fig. 7a. The observed rate constant for photodecomposition, $k_{\text{obs}} = 0.13 \pm 0.01 \text{ min}^{-1}$ ($t_{1/2} \sim 5.3 \text{ min}$; Fig. 7b).

The steady state photolyses of **1b** and **1d** were analyzed by ^1H NMR spectroscopy. Interestingly, during the photolysis of **1b**, no MeSO_2^- (diagnostic peak at 2.23 ppm) was observed as an indicator of HNO generation, Fig. 8a. Separate experiments showed that both MeSO_2^- and MeSO_2NH_2 are photostable in the same solvent mixture (2 h irradiation). Since the chemical shift of the characteristic Me peak of the expected MeSO_2NH_2 product (3.08 ppm) coincides with the chemical shift of the Me group in donor **1b**, the rate of decay of donor **1b** was monitored by the decay of the aromatic proton peak of **1b** at 8.10 ppm. A small amount of an unknown species (3.38 ppm) was also observed, which is most likely a secondary photoproduct. Control experiments showed that this peak is not from methanesulfonate (2.68 ppm), methanol (3.27 ppm) or $\text{CH}_3\text{SO}_2\text{NHOH}$ (3.07 ppm) (the photolysis sample

was spiked with these species). The observed rate constant for photodecomposition, $k_{\text{obs}} = 0.18 \pm 0.01 \text{ min}^{-1}$ ($t_{1/2} \sim 3.8 \text{ min}$; see Fig. 8b).

Finally, the steady state photolysis of **1d** was also followed by ^1H NMR spectroscopy (see Fig. 9). MeSO_2NH_2 was the only MeSO_2 -containing product observed in the photoproduct mixture. Interestingly the rate of photodecomposition for **1d** was $k_{\text{obs}} = 0.035 \pm 0.001 \text{ min}^{-1}$ ($t_{1/2} \sim 19.8 \text{ min}$ Fig. 9b), which is approximately five times slower than the rate of decomposition of **1a**, **1b** and **1c** under identical conditions.

2-Nitrosobenzaldehyde (**13**) and 4,5-dimethoxy-2-nitrosobenzaldehyde (**14**) are the other expected aromatic photoproducts arising as a result of C-O bond cleavage (Pathway 1, Scheme 4). To confirm the formation of these two species, photolyzed samples of **1a** and **1c** were analyzed by high resolution mass spectrometry (HRMS). The corresponding nitroso aldehydes **13** and **14** were observed at m/z 136.0392 (calculated mass for $[(\mathbf{13} + \text{H})]^+ = 136.0393$) and m/z 196.0604 (calculated mass for $[(\mathbf{14} + \text{H})]^+ = 196.0604$), respectively. A peak was also observed at 10.21 ppm, which was subsequently shown to be attributable to the CHO proton of **13**.

Given that O-N bond cleavage is the major pathway in each system, 2-nitrosobenzaldehyde (**15**) and 4,5-dimethoxy-2-nitrosobenzaldehyde (**16**) were initially anticipated to be the major aromatic photolysis products derived from **1a,b** and **1c,d** respectively (Pathway 2, Scheme 4). However, 2-nitrosobenzoic acid (**17**) and 4,5-dimethoxy-2-nitrosobenzoic acid (**18**) were instead identified in the photoproduct solutions by HRMS, at m/z 152.0341 (calculated mass for $[(\mathbf{17} + \text{H})]^+ = 152.0342$) and 212.0551 (calculated mass for $[(\mathbf{18} + \text{H})]^+ = 212.0533$), respectively. Others have shown that 2-

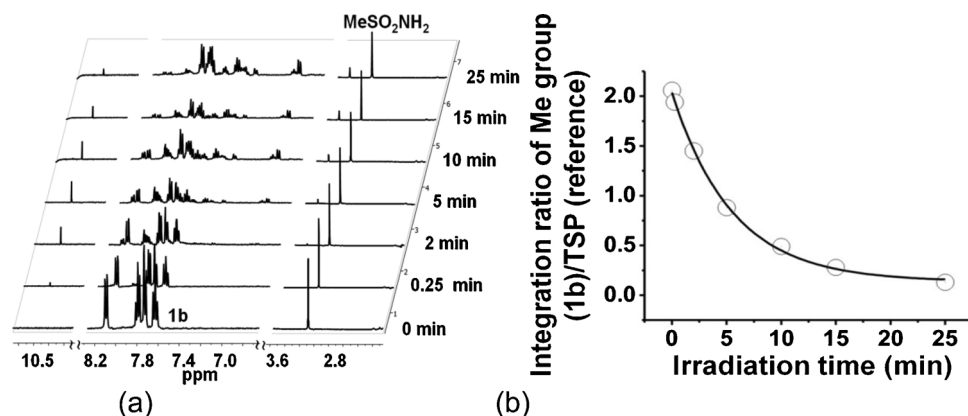


Fig. 8. (a) ^1H NMR spectra for the photodecomposition of **1b** (3.89 mM) in a mixture of phosphate buffer (0.10 mM, pH 7.00) and CD_3CN (40:60, v/v). (b) Best fit of the peak area of **1b** (aromatic H at 8.10 ppm) versus time to a first-order rate equation, giving $k_{\text{obs}} = 0.18 \pm 0.01 \text{ min}^{-1}$ ($t_{1/2} \sim 3.8 \text{ min}$).

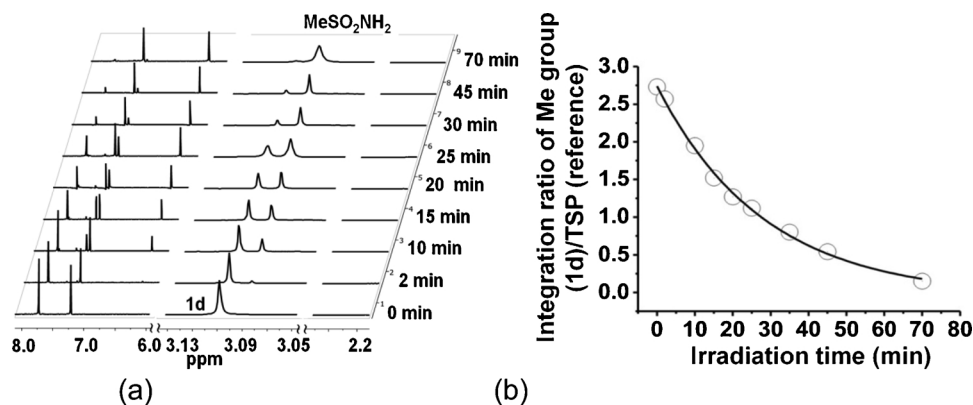


Fig. 9. (a) ^1H NMR spectra for the photodecomposition of **1d** (3.10 mM) in a mixture of phosphate buffer (0.10 mM, pH 7.00) and CD_3CN (40:60, v/v). (b) Best fit of the peak area of **1d** (MeSO_2 signal) versus time to a first-order rate equation, giving $k_{\text{obs}} = 0.035 \pm 0.001 \text{ min}^{-1}$ ($t_{1/2} \sim 19.8 \text{ min}$).

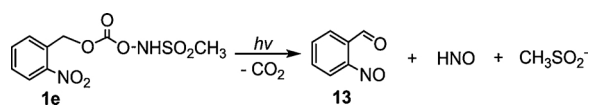


Fig. 10. Proposed HNO generation pathway for the photolysis of compound **1e**.

nitrosobenzaldehyde is photoactive and decomposes to generate nitrosobenzoic acid upon irradiation [85–89]. To confirm that nitro aldehydes **15** and **16** are indeed unstable upon irradiation, authentic samples of **15** and **16** were irradiated using the same experimental setup in the identical solvent mixture. As shown in Fig. S6 and S7 in the Supporting Information, nitroso acid **17** was obtained from the anaerobic photolysis of nitro aldehyde **15**. Anaerobic photolysis of nitro aldehyde **16** yielded nitroso acid **18**. Hence nitroso acids, not nitro benzaldehydes, are observed in the photoproduct mixture, due to the photosensitivity of the latter compounds. Photolyzed nitro aldehydes are efficiently converted to nitroso acids **17** and **18** via a ketene intermediate [89].

The desired HNO generation pathway for the photolysis of **1e** is shown in Fig. 10. The photocoupling of the NB group was expected to release HNO and MeSO_2^- with the elimination of CO_2 , where HNO generation was inferred by the release of MeSO_2^- . The chromophore generated during the primary photolysis was anticipated to be 2-nitrosobenzaldehyde (**13**). Photodecomposition of target **1e** in a 60:40 mixture of CD_3CN and phosphate buffer (0.10 M, pH 7.0) under anaerobic conditions with monitoring by ^1H NMR analysis (see Fig. 11a), revealed the formation of MeSO_2NHOH (3.05 ppm, 71%), MeSO_2^- (2.23 ppm, 11%, HNO generation pathway), MeSO_3^- (2.71 ppm, 8%), and MeSO_2NH_2 (3.08 ppm, 10%) after irradiation for 170 min. The

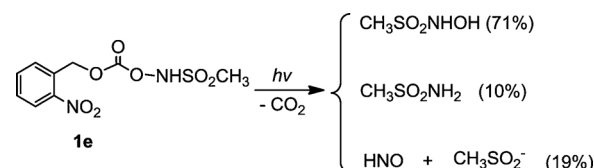


Fig. 12. Observed photolytic pathway for compound **1e**.

characteristic peak of 2-nitrosobenzaldehyde was observed at 10.21 ppm. In a separate experiment the photolysis product solution of a partially photolyzed solution of **1e** was taken to dryness and the ^1H NMR spectrum was recorded in CHCl_3 . The resulting spectra revealed resonances at δ 12.08 (s), 7.89 (dt), and 6.43 (dd) that are consistent with literature values for **13** in the same solvent [57]. The remaining expected peaks for **13** overlapped with peaks from the reactant. Again, by monitoring the decay of the integration of the CH_3 signal (^1H NMR) in **1e**, a first-order rate constant $k_{\text{obs}} = 0.024 \pm 0.002 \text{ min}^{-1}$ is observed with a half-life $\sim 28.9 \text{ min}$ (see Fig. 11b). MeSO_3^- was found to be derived from a subsequent oxidation of MeSO_2^- , presumably due to the presence of traces of molecular oxygen as an adventitious oxidizing agent. Thus, $\sim 19\%$ HNO generation from the photolysis of **1e** was inferred by both MeSO_2^- and MeSO_3^- formation. The photolytic pathway observed in the photolysis of **1e** is summarized in Fig. 12.

2.3. Determination of the Photoproduct Quantum Yields of 1a-1e

The photoproduct quantum yields of compounds **1a-1e** were determined by actinometry at $313 (\pm 3) \text{ nm}$, with *trans*-azobenzene used

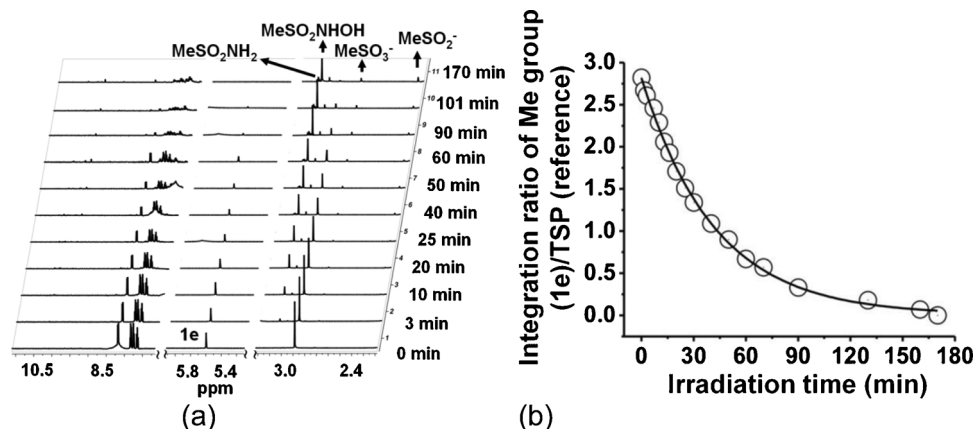
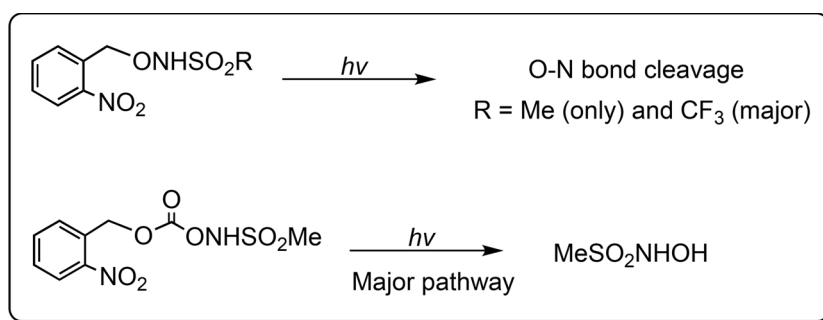


Fig. 11. (a) ^1H NMR spectra for the photodecomposition of **1e** (3.89 mM) in a 60:40 (v/v) mixture of CD_3CN and phosphate buffer (0.10 M, pH 7.00). (b) Best fit of the CH_3 peak area versus time to a first-order rate equation, giving $k_{\text{obs}} = 0.024 \pm 0.002 \text{ min}^{-1}$ ($t_{1/2} \sim 28.9 \text{ min}$).

as a reference compound ($\Phi_{(trans \rightarrow cis)} = 0.14$ [90]; see Experimental Section and Figures S8-S13). Photochemical reactions must be zero-order with respect to the reactant for accurate determination of quantum yields. A control experiment with our MeSO₂-based substrate **1b** showed that the photoproducts and the observed rate constant for decomposition are not affected by the concentration of **1b** (Fig. S14, Supporting Information). The percentage of *trans*-azobenzene converted to *cis*-azobenzene upon irradiation was followed by UV-vis spectroscopy, whereas the photodecomposition of **1a-1e** was followed by NMR spectroscopy (¹⁹F or ¹H). The photoproduct quantum yields were 0.67 ± 0.03 (**1a**), 0.77 ± 0.03 (**1b**), 0.46 ± 0.02 (**1c**), 0.27 ± 0.01 (**1d**), and 0.23 ± 0.01 (**1e**), respectively. Photoproduct quantum yield values for **1a** (0.67 ± 0.03) and **1b** (0.77 ± 0.03) are higher compared to structurally related nitrobenzyl systems ($\Phi = 0.49$ for 2-nitrobenzyl methyl ether [57]), with the leaving group affecting the photoproduct quantum yield [51]. The similarity in the quantum yield values for **1a** and **1b** is expected, since the compounds are structurally similar and the observed rate constants for **1a** ($0.22 \pm 0.01 \text{ min}^{-1}$) and **1b** ($0.18 \pm 0.01 \text{ min}^{-1}$) were comparable. The photoproduct quantum yields of **1c** (0.46 ± 0.02) and **1d** (0.27 ± 0.01) are lower as a result

release of benzohydroxamic acid from a nitrobenzyl photoprotected conjugate, and postulated that O-N bond homolysis occurs [75]. Irradiation at a shorter wavelength favored O-N bond cleavage, whereas irradiation at longer wavelength favored C-O bond cleavage. The photoproducts from irradiation of **1a-1d** at two different excitation wavelengths were therefore investigated, using a xenon lamp in conjunction with a monochromator. The results are summarized in Table S2 in the Supporting Information. The excitation wavelength did not have any effect on the observed photoproducts. The importance of the nitro group on photodecomposition for this family of molecules was also investigated, by studying the steady state photodecomposition of the structurally related compound (*N*-benzyloxy-1,1,1-trifluoromethanesulfonamide (**19**) which lacks the *o*-nitro substituent. There was essentially no photodecomposition of **19** even after irradiation for 6 h at 300 nm in the solvent mixture of phosphate buffer (pH 7.00, 5.0 mM) and CD₃CN (0.45 mL, 40:60, v/v) (Fig. S15); hence the nitro functional group plays a key role in the photoactivity of molecules **1a-1e**; that is, both C-O and O-N bond cleavage pathways are dependent on the presence of this group.



of the electron-donating MeO substituents on the aromatic group, which significantly reduce the photoproduct quantum yields for nitrobenzyl-caged molecules [91–92]. The significantly lower observed rate constant for photodecomposition upon steady state irradiation of **1d** ($k_{\text{obs}} = 0.035 \text{ min}^{-1}$) and **1e** ($k_{\text{obs}} = 0.024 \text{ min}^{-1}$) compared with **1a-1c** ($k_{\text{obs}} = 0.22, 0.18$ and 0.13 min^{-1} , respectively) is attributed to the lower photoproduct quantum yield for **1d** and **1e** (0.27 ± 0.01 (**1d**), and 0.23 ± 0.01 (**1e**)).

3. Further Studies to Probe the Photolysis Reaction Mechanisms

Numerous mechanistic studies have been carried out on the photodecomposition of molecules of the type *o*-NO₂Bn-O-X, where O-X bond cleavage occurs [51,75,81]. Detailed mechanistic studies on the photodecomposition of 1-(methoxymethyl)-2-nitrobenzene provide support for intramolecular 1,5-hydrogen transfer in the excited state leading to formation of a ground state quinonoid *aci*-nitro tautomer within 5 ps [57]. The monoprotonated *aci*-nitro intermediate cyclizes to form a benzisoxazolidine species followed by a 1,3-hydrogen shift to give the corresponding hemiacetal *via* ring opening [57]. Hydrolysis leads to the release of the protonated leaving group (MeOH), and 2-nitrosobenzaldehyde [57]. Multiple isomers exist for several of the intermediates [51]. For poor leaving groups such as MeO⁻, the last step is the rate-determining step, occurring on the millisecond timescale ($k = 2.5 \times 10^{-2} \text{ s}^{-1}$; $t_{1/2} \sim 36 \text{ ms}$) [57]. The rate constant for the loss of the leaving group depends on the solvent, pH, and the nature of the leaving group [57,93–94].

Although light-induced O-N bond cleavage has previously been observed for *o*-NO₂Bn-O-N- systems [75], little is known about the mechanism of this reaction. McCulla et al. studied the photoinduced

Studies were also carried out to determine whether the solvent ratio and/or the pH of the aqueous component of the solvent altered the amount of C-O versus O-N bond cleavage for **1b**. The selectivity for C-O versus O-N bond cleavage was highly dependent on the solvent ratio (CH₃CN : phosphate buffer) for related photocaged *N*-hydroxysulfonamides [46–47, 49]. The rate and products of photolysis of **1b** were investigated at various CH₃CN : phosphate buffer (5.0 mM) solvent ratios (Fig. S16). The results are summarized in Table S3 in the Supporting Information. Only O-N, not C-O bond cleavage, was observed at all solvent ratios. The observed rate constant was independent of the solvent ratio.

In previous studies, the pH of the solution was found to affect the observed rate of photodecomposition of *o*-nitrobenzyl compounds which decompose via C-O bond cleavage [57, 93–94]. Specifically, the rate of cyclization of the *aci*-nitro intermediate to the 1,3-dihydrobenz[*c*]isoxazol-1-ol intermediate, the formation of hemiacetal intermediate *via* ring opening and the hydrolysis of hemiacetal intermediate were pH-dependent processes [57]. The effect of the pH of the aqueous component in the solvent mixture was investigated on the photodecomposition of **1b** (Fig. S17), to determine whether pH could influence the selectivity for C-O versus O-N bond cleavage. The results are summarized in Table S4 in the Supporting Information. Varying the pH of the aqueous component has no effect on the observed rate constant for photodecomposition or the nature of photolytic products derived from **1b**, with only O-N bond cleavage occurring.

The photolysis data reported thus far were all obtained under anaerobic conditions. To probe the effect of oxygen on the mechanism of the reaction, the photodecomposition of **1b** was also studied under aerobic conditions. The ¹H NMR spectrum of the photoproducts was identical to that observed under anaerobic conditions. The observed rate

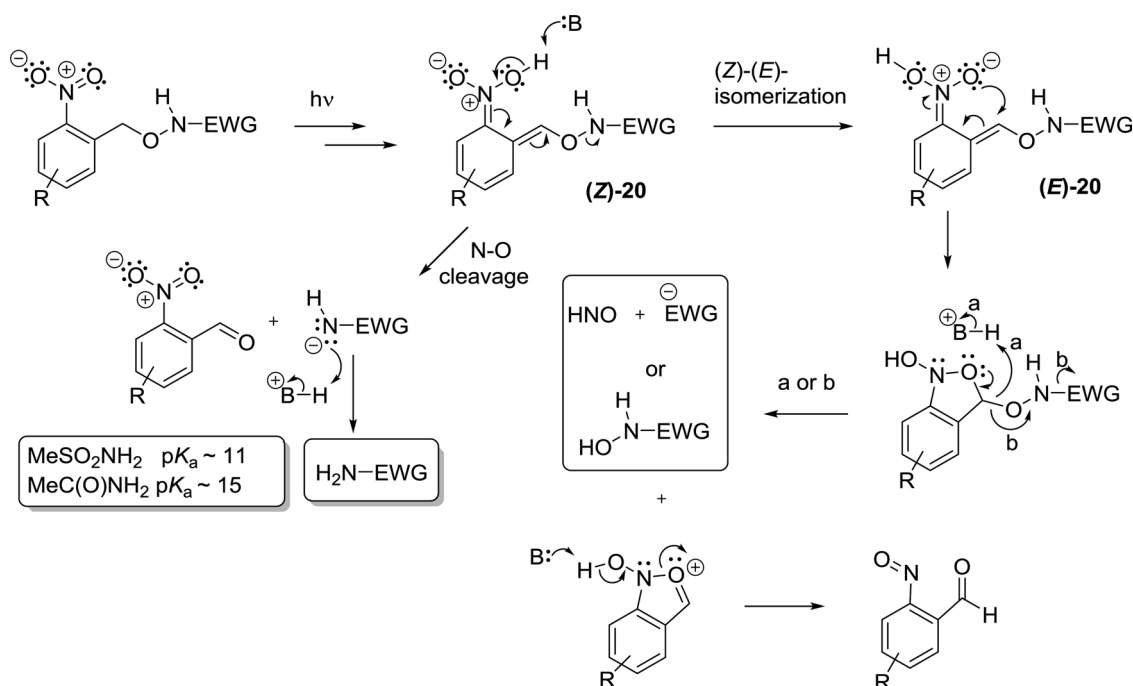


Fig. 13. Proposed mechanism for photolysis of NB-caged substrates **1a-1d**.

constant (k_{obs}) for the photolysis was $0.20 \pm 0.03 \text{ min}^{-1}$ ($t_{1/2} \sim 3.3 \text{ min}$) under aerobic conditions (see Fig. S18a), which is the same as that obtained under anaerobic conditions (Fig. S18b; $0.20 \pm 0.03 \text{ min}^{-1}$ ($t_{1/2} \sim 3.3 \text{ min}$)). Ultrafast spectroscopy experiments are required to determine whether O-N bond cleavage occurs via the singlet and/or triplet excited states.

Qvortrup et al. recently reported solvent-controlled photorelease of hydroxamic acids bearing the NB PCG. Whereas C-O bond cleavage occurred in protic solvents, release of a carboxamide occurred via O-N bond cleavage in aprotic solvents [81]. In stark contrast, in the present study conducted in *protic* medium, C-O cleavage (HNO generation) (Pathway 1, Scheme 4) is only a minor photolysis pathway for **1a** and **1c**, and the competing O-N cleavage pathway dominates (> 90%). It should be noted that the parent HNO donor ($\text{CF}_3\text{SO}_2\text{NHO}(\text{H})$) was not observed by ^{19}F NMR spectroscopy during the photolysis of **1a** and **1c**. Given that the half-life for decomposition of $\text{CF}_3\text{SO}_2\text{NHO}(\text{H})$ is $\sim 10 \text{ min}$ [18], the absence of $\text{CF}_3\text{SO}_2\text{NHO}(\text{H})$ as a reaction intermediate in the ^{19}F NMR spectra suggests that C-O bond cleavage and the release of CF_3SO_2^- are concerted processes in the minor pathway operating with these substrates.

No evidence for operation of the HNO generation pathway was obtained upon photolysis of **1b** and **1d**. For these compounds only O-N bond cleavage (Pathway 2, Scheme 4) was observed. Although CF_3SO_2^- is a better leaving group than MeSO_2^- as indicated by their conjugate acid $\text{p}K_a$ values ($\text{p}K_a(\text{MeSO}_2\text{H}) = 2.28$ and $\text{p}K_a(\text{CF}_3\text{SO}_2\text{H}) = -0.6$) [47], there is little difference in selectivity for the competing photolysis pathways for the CF_3SO_2^- -containing and CH_3SO_2^- -containing analogs **1a-1d**.

Photochemical O-N bond scission is a commonly observed pathway in many hydroxamic acid and alkyl hydroxamate systems [95–96]; however, as mentioned earlier, Qvortrup noted that the photolytic release of hydroxamic acids caged by the NB PCG was observed via C-O cleavage in protic solvents in high yield [80–81], while competing N-O bond cleavage leading to carboxamides was observed in aprotic solvents [81]. Based on an examination of the mechanistic insights for these competing C-O and O-N cleavage pathways proffered by Qvortrup, we hypothesize that the reversal in selectivity for C-O vs N-O bond cleavage in protic media with our substrates **1a-1d** is due to the presence of the better sulfonamido leaving group in **1a-1d** relative to

the carboxamido leaving group of the Qvortrup systems (see Fig. 13). The sulfonamido moieties are clearly better leaving groups as evidenced by their $\text{p}K_a$ values: $\text{CF}_3\text{SO}_2\text{NH}_2$ ($\text{p}K_a = 6.33$ (H_2O) [97]; 9.7 (DMSO) [98]), $\text{CH}_3\text{SO}_2\text{NH}_2$ ($\text{p}K_a = 10.8$ (H_2O) [97]; 17.5 (DMSO) [98]) and $\text{CH}_3\text{C}(\text{O})\text{NH}_2$ ($\text{p}K_a = 15.1$ (H_2O) [99]; 25.5 (DMSO) [98]). Therefore, depending on the solvent, the sulfonamide NH proton is approximately 10^4 to 10^8 times more acidic than the analogous carboxamide proton. With a weaker (amide) leaving group, Qvortrup observed protic solvent-mediated (Z)-(E) isomerization of *aci*-nitro intermediate (Z)-20 to (E)-20, leading to cyclization and then C-O cleavage as the dominant pathway. In our system, we hypothesize that rapid O-N cleavage with loss of a (better) sulfonamide leaving group occurs before there is an opportunity for the (Z)-(E) isomerization to (E)-20 needed for C-O cleavage. This is consistent with this pathway exhibiting no dependence on either the solvent ratio or the pH of the aqueous component of the solvent mixture.

In contrast, the carbonate-linked CH_3SO_2^- -derivative **1e** generated mainly the parent HNO donor $\text{CH}_3\text{SO}_2\text{NHO}(\text{H})$ (71%) via C-O bond cleavage (path a), along with a small quantity of HNO (diagnosed by the presence MeSO_2^-) presumably formed via a concerted mechanism (path b) and MeSO_2NH_2 formed via a direct O-N bond cleavage (Fig. 14). Control experiments demonstrated that $\text{CH}_3\text{SO}_2\text{NHO}(\text{H})$ is stable in the protic solvent mixture used for these studies due to its high $\text{p}K_a$ value (9.95 [18]), which precludes direct deprotonation and subsequent decomposition of $\text{CH}_3\text{SO}_2\text{NHO}(\text{H})$ to yield MeSO_2^- . Therefore, any $\text{CH}_3\text{SO}_2\text{NHO}^-$ formed from the photolysis of **1e** would be rapidly protonated to form $\text{CH}_3\text{SO}_2\text{NHO}(\text{H})$ under our photolytic conditions (pH 7.0); the small amount of MeSO_2^- must then form via a minor competing concerted decomposition pathway. The formation of small amounts of MeSO_2NH_2 results from competing O-N bond cleavage. The dramatic change in selectivity here vis-à-vis substrates **1a-1d** is likely due to the more enthalpically demanding bond cleavage requirements necessary for ultimate N-O cleavage. This presumably allows for competition from (Z)-(E)-isomerization of the *aci*-nitro intermediate **21** which permits the C-O cleavage pathway to dominate.

4. Conclusions

A novel family of *o*-nitrobenzyl-caged *N*-hydroxysulfonamides **1a-**

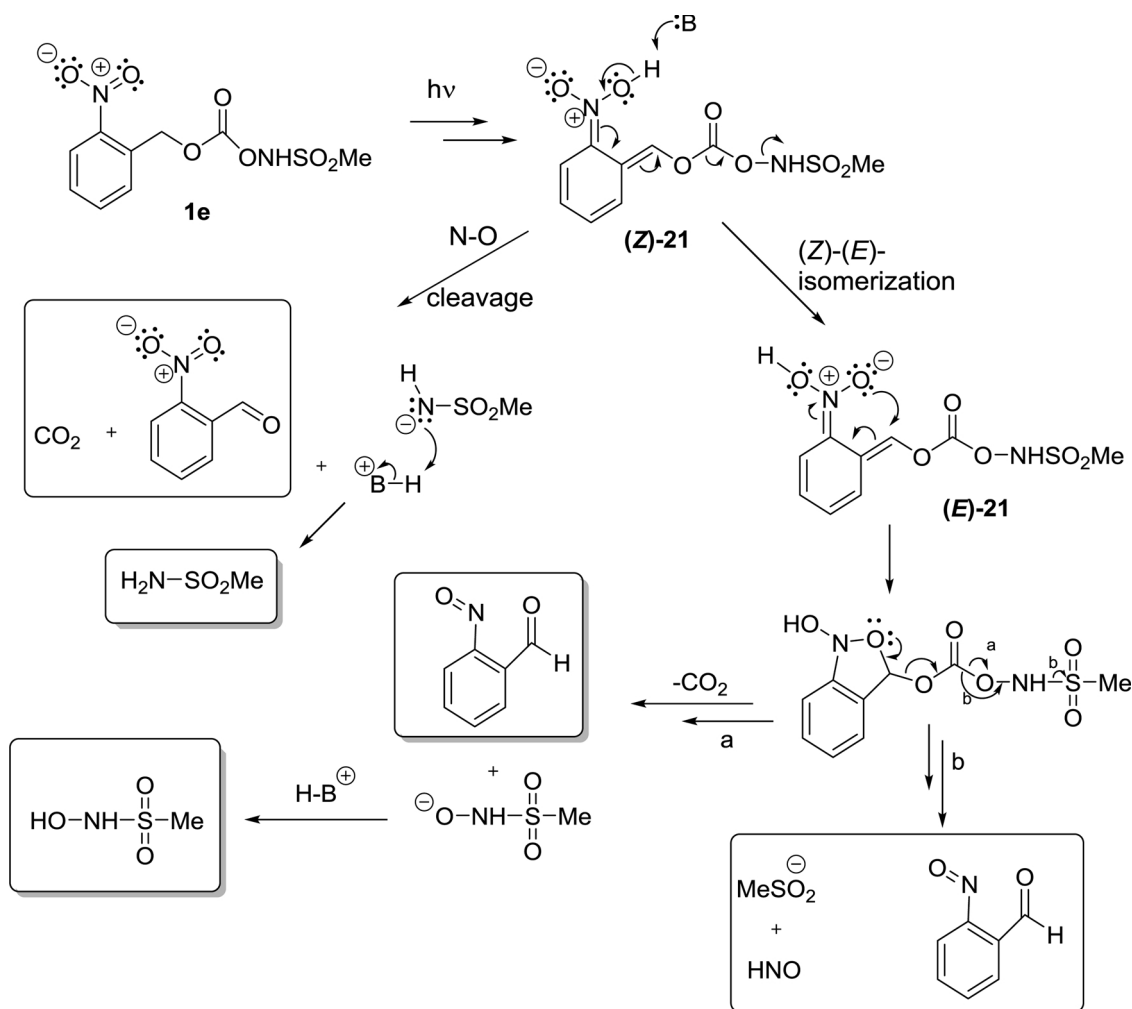


Fig. 14. Proposed mechanism for photolysis of carbonate-linked NB-caged substrate **1e**.

1e have been synthesized. Upon steady-state irradiation (300 nm), photochemical decomposition of **1a-1e** occurs within minutes. The desired HNO generation pathway was observed only as a minor pathway for compounds **1a** and **1c**, where a competing photoinduced O-N bond cleavage pathway was the major pathway. Only the O-N cleavage pathway was observed for **1b** and **1d**. The presence or absence of methoxy groups on the *o*-nitrophenyl ring has minimal influence on the C-O versus O-N bond cleavage selectivity, and similar results are seen for both methane- and trifluoromethane-sulfonamidoxy substrates. However, the *o*-nitro substituent plays an essential role in photodecomposition. In contrast, with the analogous carbonate linked substrate **1e**, the release of parent HNO donor $\text{CH}_3\text{SO}_2\text{NHOH}$ was observed as the major pathway. A concerted MeSO_2^- -releasing decomposition pathway and O-N bond cleavage were observed as only minor pathways in this system. For **1b**, only O-N bond cleavage occurred regardless of the solvent ratio, the pH of the aqueous component and the absence or presence of oxygen.

The selectivity for O-N cleavage during the photolysis of **1b** represents a complete switch in photolysis mechanism relative to the analogous *o*-nitrobenzyl carboxamidoxy substrates reported by McCulla and Qvortrup. Therefore, future studies will further probe the mechanism of N-O bond cleavage of **1b** using laser flash photolysis. The promise of such *o*-nitrobenzylsulfonamides as potential N-protecting groups for a range of sulfonamides will also be explored.

5. Experimental Section

5.1. General Information

Except where specifically stated, commercially obtained chemicals were used without purification. Commercially available anhydrous pyridine, *N,N*-dimethylformamide (DMF) and dimethyl sulfoxide (DMSO) were used without purification. Tetrahydrofuran (THF) was distilled over Na and benzophenone, and CH_2Cl_2 was distilled from CaH_2 . All reactions were set up using anhydrous organic solvents under an inert atmosphere. Silica gel (60 Å, 40 - 63 μm) and ACS grade solvents (ethyl acetate, petroleum ether (boiling point range: 30 - 60 °C) and CH_2Cl_2) were used for column chromatography. Based-treated silica chromatography columns were made by making a silica slurry using a solvent mixture of 5% Et_3N and 95% petroleum ether followed by washing with petroleum ether to remove excess Et_3N after loading the column. All synthetic products were characterized by ^1H , ^{13}C and ^{19}F NMR spectroscopy, and high-resolution mass spectrometry (HRMS) with a direct analysis in real time (DART) ion source. ^1H , ^{13}C and ^{19}F NMR spectra were recorded using a Bruker 400 MHz spectrometer with a 5 mm probe at 25 ± 1 °C. All NMR spectra were analyzed using MestReNova (version 11.3) software.

KH_2PO_4 was used to prepare the phosphate buffer solution (0.10 M and 5.0 mM, pH 7.00). The pH of the buffer was adjusted with NaOH (0.10 M) solution with monitoring using an Orion Model 710A pH meter equipped with Mettler-Toledo Inlab 423 or 421 electrodes at room temperature. After degassing with argon for ~ 24 h, the

phosphate buffer solution was stored in a MBRAUN Labmaster 130 (1250/78) glovebox equipped with O₂ and H₂O sensors under an argon atmosphere.

5.2. Synthetic procedures and product characterization

5.2.1. 2-(2-Nitrobenzyloxy)isoindoline-1,3-dione (**3a**)

A solution of 2-nitrobenzyl bromide (**2a**) (5.01 g, 23.2 mmol) in anhydrous DMF (40 mL) was added dropwise at room temperature to a stirred solution of *N*-hydroxyphthalimide (4.15 g, 25.4 mmol) and *N,N*-diisopropylethylamine (DIEA, 4.43 mL, *d* = 0.742 g/mL at 25 °C, 25.4 mmol) in anhydrous DMF (60 mL) under N₂. The reaction mixture was heated to 70 °C (over 30 min) and was stirred for 2 h. The reaction mixture was allowed to cool to room temperature and was then poured into water (200 mL). The aqueous layer was extracted with ethyl acetate (3 × 100 mL). A pale-yellow solid precipitated between the aqueous and organic phases, which was separated by filtration. The pale-yellow solid was washed with ethyl acetate (100 mL) and dried under vacuum to give a pale-yellow solid (4.67 g), which was identified as pure product **3a**. The combined organic extracts were dried over MgSO₄, filtered and concentrated *in vacuo* to afford a yellow solid. This crude product was purified by column chromatography (silica gel/15:85 ethyl acetate-petroleum ether) to obtain a second fraction of the title product **3a** (1.73 g). Overall, the title compound **3a** was obtained as a yellow solid (6.40 g, 93%). m.p. 168–171 °C. ¹H NMR (400 MHz, DMSO-*d*₆) δ 8.11 (dd, *J* = 7.6, 1.2 Hz, 1 H), 7.89 (dd, *J* = 7.6, 1.2 Hz, 1 H), 7.90–7.76 (m, 4 H), 7.78 (td, *J* = 7.6, 1.2 Hz, 1 H), 7.66 (td, *J* = 7.6, 1.2 Hz, 1 H), 5.55 (s, 2 H). ¹³C NMR (101 MHz, DMSO-*d*₆) δ 162.83, 147.92, 134.69, 133.71, 131.26, 130.04, 129.78, 128.34, 124.67, 123.15, 75.28. HRMS *m/z* (DART) calculated for MH⁺ 299.0662, found 299.0660.

5.2.2. 2-(4,5-Dimethoxy-2-nitrobenzyloxy)isoindoline-1,3-dione (**3b**)

A solution of 4,5-dimethoxy-2-nitrobenzyl bromide (**2b**) (4.500 g, 16.30 mmol) in anhydrous DMF (40 mL) was added dropwise at room temperature to a stirred solution of *N*-hydroxyphthalimide (3.000 g, 18.39 mmol) and *N,N*-diisopropylethylamine (DIEA, 3.40 mL, *d* = 0.742 g/mL at 25 °C, 19.5 mmol) in anhydrous DMF (40 mL), under N₂. The reaction mixture was heated to 70 °C (over 30 min) and was stirred at 70 °C for 7.5 h. The reaction mixture was allowed to cool to room temperature and was then poured into water (300 mL). The aqueous layer was extracted with ethyl acetate (3 × 150 mL). A yellow solid precipitated between the aqueous and organic phases, which was separated by filtration. This yellow solid was washed with ethyl acetate (100 mL) and dried under vacuum, to yield pure title compound **3b** (3.56 g) as a yellow solid. The combined organic extracts were dried over MgSO₄, filtered and concentrated *in vacuo* to afford a yellow solid. This crude product was purified by column chromatography (silica gel/30:70 ethyl acetate-petroleum ether) to obtain a second fraction of the title compound **3b** (1.95 g). Overall, the title compound **3b** was obtained as a yellow powder (5.51 g, 94%). m.p. 199–200 °C. ¹H NMR (400 MHz, DMSO-*d*₆) δ 7.84 (s, 4 H), 7.68 (s, 1 H), 7.53 (s, 1 H), 5.55 (s, 2 H), 3.89 (s, 3 H), 3.88 (s, 3 H). ¹³C NMR (101 MHz, DMSO-*d*₆) δ 163.12, 152.74, 148.32, 140.46, 134.81, 128.51, 125.01, 123.28, 112.89, 108.12, 75.54, 56.29, 56.11. HRMS *m/z* (DART) calculated for MH⁺ 359.0874, found 359.0874.

5.2.3. *O*-(2-Nitrobenzyl)hydroxylamine (**4a**)

Hydrazine monohydrate (0.567 mL, *d* = 1.032 g/mL at 25 °C, 11.7 mmol) was added in one portion to a stirred solution of **3a** (1.73 g, 5.80 mmol) in anhydrous CH₂Cl₂ (120 mL) under N₂ at room temperature. The reaction mixture was stirred for 4 h at room temperature. After the resulting white suspension was filtered off, the filtrate was washed with water (100 mL). The aqueous layer was extracted with CH₂Cl₂ (3 × 80 mL) and the combined organic extracts were dried over MgSO₄ and concentrated *in vacuo*. The title compound **4a** was obtained

as a yellow oil (0.90 g, 92%), which was pure and was directly used in the next step. ¹H NMR (400 MHz, DMSO-*d*₆) δ 8.02 (dd, *J* = 8.0, 1.2 Hz, 1 H), 7.77–7.70 (m, 2 H), 7.56 (td, *J* = 8.0, 1.6 Hz, 1 H), 6.26 (s, 2 H), 4.89 (s, 2 H). ¹³C NMR (101 MHz, DMSO-*d*₆) δ 147.69, 134.09, 133.48, 129.41, 128.40, 124.24, 73.08. HRMS *m/z* (DART) calculated for MH⁺ 169.0608, found 169.0607.

5.2.4. *O*-(4,5-Dimethoxy-2-nitrobenzyl)hydroxylamine (**4b**)

Hydrazine monohydrate (1.24 mL, *d* = 1.032 g/mL at 25 °C, 25.6 mmol) was added in one portion to a stirred solution of **3b** (3.780 g, 10.55 mmol) in anhydrous CH₂Cl₂ (120 mL) under N₂ at room temperature. The reaction mixture was stirred for 4 h at room temperature. After the resulting white suspension was filtered off, the filtrate was washed with water (100 mL). The aqueous layer was extracted with CH₂Cl₂ (3 × 80 mL) and the combined organic extracts were dried over MgSO₄, filtered, and concentrated *in vacuo*. The title compound **4b** was obtained as a yellow oil (2.05 g, 85%), which was pure and was directly used in the next step. ¹H NMR (400 MHz, DMSO-*d*₆) δ 7.65 (s, 1 H), 7.19 (s, 1 H), 6.33 (s, 2 H), 4.90 (s, 2 H), 3.86 (s, 3 H), 3.85 (s, 3 H). ¹³C NMR (101 MHz, DMSO-*d*₆) δ 153.18, 147.21, 139.35, 129.89, 110.26, 107.71, 73.36, 56.05, 55.90. HRMS *m/z* (DART) calculated for MH⁺ 229.0819, found 229.0819.

5.2.5. 1,1,1-Trifluoro-*N*-(2-nitrobenzyloxy)methanesulfonamide (**1a**)

A solution of trifluoromethanesulfonyl chloride (0.683 mL, *d* = 1.583 g/mL at 25 °C, 6.42 mmol) in anhydrous CH₂Cl₂ (2.0 mL) was added dropwise over 3 min at -25 °C to a stirred solution of **4a** (831.2 mg, 4.943 mmol), 4-(*N,N*-dimethylamino)pyridine (DMAP, 302.1 mg, 2.473 mmol) and anhydrous pyridine (0.40 mL, *d* = 0.978 g/mL at 25 °C, 4.9 mmol), in anhydrous CH₂Cl₂ (10 mL) under N₂. The reaction mixture was allowed to warm to room temperature over 30 min. After stirring for 4 h at room temperature, the reaction mixture was washed with saturated aqueous CuSO₄ solution (100 mL), and the aqueous layer was extracted with CH₂Cl₂ (3 × 100 mL). The combined organic extracts were dried over MgSO₄, filtered, and concentrated *in vacuo*. The resulting crude oil was purified by column chromatography (silica gel/2:98 MeOH-CH₂Cl₂) to give the title product **1a** as a colorless oil (599.43 mg, 40%). ¹H NMR (400 MHz, CDCl₃) δ 8.11 (dd, *J* = 7.6, 1.2 Hz, 1 H), 7.69 (td, *J* = 7.6, 1.2 Hz, 1 H), 7.61–7.55 (m, 2 H), 5.46 (s, 2 H). ¹³C NMR (101 MHz, CDCl₃) δ 148.08, 133.82, 130.79, 129.92, 129.69, 125.23, 119.23 (q, *J* = 325 Hz), 77.06. ¹⁹F NMR (376 MHz, CDCl₃) δ -73.36. HRMS *m/z* (DART) calculated for MH⁺ 301.0101, found 301.0103.

5.2.6. *N*-(2-Nitrobenzyloxy)methanesulfonamide (**1b**)

A solution of methanesulfonyl chloride (0.205 mL, *d* = 1.48 g/mL at 25 °C, 2.65 mmol) in anhydrous CH₂Cl₂ (2.5 mL) was added dropwise at -20 °C to a stirred solution of **4a** (446.56 mg, 2.6557 mmol), DMAP (326.9 mg, 2.676 mmol) and anhydrous pyridine (0.214 mL, *d* = 0.978 g/mL at 25 °C, 2.65 mmol), in anhydrous CH₂Cl₂ (25 mL) under N₂. The reaction mixture was allowed to warm to room temperature over 30 min. After stirring for another 1 h at room temperature, the reaction mixture was washed with saturated aqueous CuSO₄ solution (70 mL), and the aqueous layer was extracted using CH₂Cl₂ (3 × 50 mL). The combined organic extracts were dried over MgSO₄ and concentrated *in vacuo*. The resulting crude oil was purified by column chromatography (silica gel/30:70 ethyl acetate-petroleum ether) to give the title product **1b** as a yellow powder (152.40 mg, 23%). In addition, *bis*-methanesulfonation product **5** was also isolated as a pale yellow solid (118.86 mg, 14%). Characterization of **1b**: m.p. 77–79 °C. ¹H NMR (400 MHz, CDCl₃) δ 8.06 (dd, *J* = 7.6, 1.2 Hz, 1 H), 7.67 (td, *J* = 7.6, 1.2 Hz, 1 H), 7.60 (dd, *J* = 7.6, 1.2 Hz, 1 H), 7.54 (td, *J* = 8.0, 1.6 Hz, 1 H), 7.08 (br s, 1 H), 5.40 (s, 2 H), 3.09 (s, 3 H). ¹³C NMR (101 MHz, CDCl₃) δ 148.42, 133.50, 131.23, 130.61, 129.64, 125.01, 75.97, 37.12. HRMS *m/z* (DART) calculated for MH⁺ 247.0383, found 247.0381. Characterization of **5**: ¹H NMR (400 MHz,

DMSO- d_6) δ 8.13 (dd, $J = 8.0, 1.2$ Hz, 1 H), 7.83-7.78 (m, 2 H), 7.69 (td, $J = 8.0, 2.0$ Hz, 1 H), 5.48 (s, 2 H), 3.47 (s, 6 H).

5.2.7. *N*-(4,5-Dimethoxy-2-nitrobenzyloxy)-1,1,1-trifluoromethanesulfonamide (**1c**)

A solution of trifluoromethanesulfonyl chloride (0.385 mL, $d = 1.583$ g/mL at 25 °C, 3.62 mmol) in anhydrous CH_2Cl_2 (3.0 mL) was added dropwise at -27 °C to a stirred solution of **4b** (635.2 mg, 2.784 mmol), DMAP (167.0 mg, 1.367 mmol) and anhydrous pyridine (0.223 mL, $d = 0.978$ g/mL at 25 °C, 2.76 mmol), in anhydrous CH_2Cl_2 (25 mL) under N_2 . The reaction mixture was allowed to warm to room temperature over 30 min. After stirring for another 3.5 h at room temperature, the reaction mixture was washed with saturated aqueous CuSO_4 solution (80 mL), and the aqueous layer was extracted using CH_2Cl_2 (3×80 mL). The combined organic extracts were dried over MgSO_4 , filtered, and concentrated *in vacuo*. The resulting crude oil was purified by column chromatography (silica gel/2:98 MeOH- CH_2Cl_2) to give the title product **1c** as a yellow powder (342.5 mg, 34%). m.p. 120-123 °C. ^1H NMR (400 MHz, CDCl_3) δ 7.70 (s, 1 H), 7.02 (s, 1 H), 5.45 (s, 2 H), 3.99 (s, 3 H), 3.96 (s, 3 H). ^{13}C NMR (101 MHz, CDCl_3) δ 153.39, 148.95, 140.54, 124.45, 119.40 (q, $J = 326$ Hz), 111.97, 108.31, 77.34, 56.51, 56.47. ^{19}F NMR (376 MHz, CDCl_3) δ -73.45. HRMS m/z (DART) calculated for MH^+ 361.0312, found 361.0308.

5.2.8. *N*-(4,5-Dimethoxy-2-nitrobenzyloxy)methanesulfonamide (**1d**)

A solution of methanesulfonyl chloride (0.121 mL, $d = 1.48$ g/mL at 25 °C, 1.56 mmol) in anhydrous CH_2Cl_2 (3.0 mL) was added dropwise at -23 °C to a stirred solution of **4b** (275.0 mg, 1.205 mmol), DMAP (73 mg, 0.60 mmol) and anhydrous pyridine (96 μL , $d = 0.978$ g/mL at 25 °C, 1.2 mmol), in anhydrous CH_2Cl_2 (25 mL) under N_2 . The reaction mixture was allowed to warm to room temperature over 30 min. After stirring for another 4 h, the reaction mixture was washed with saturated aqueous CuSO_4 solution (90 mL), and the aqueous layer was extracted using CH_2Cl_2 (3×80 mL). The combined organic extracts were dried over MgSO_4 , filtered, and concentrated *in vacuo*. The resulting crude oil was purified by column chromatography (silica gel/40:60 ethyl acetate-petroleum ether) to give the title product **1d** as a yellow powder (327.5 mg, 89%). m.p. 136-138 °C. ^1H NMR (400 MHz, CDCl_3) δ 7.69 (s, 1 H), 7.08 (s, 1 H), 7.03 (s, 1 H), 5.38 (s, 2 H), 4.01 (s, 3 H), 3.97 (s, 3 H), 3.10 (s, 3 H). ^{13}C NMR (101 MHz, CDCl_3) δ 153.20, 148.88, 140.89, 125.31, 112.86, 108.33, 76.28, 56.62, 56.46, 37.22. HRMS m/z (DART) calculated for MH^+ 307.0594, found 307.0594.

5.2.9. *t*-Butyl-*N*-(*o*-nitrobenzyloxycarbonyloxy)carbamate (**9**)

Anhydrous pyridine (1.6 mL, $d = 0.978$ g/mL at 25 °C, 20 mmol) was added dropwise at 1 °C to a stirred mixture of 2-nitrobenzyl alcohol (3.02 g, 19.7 mmol) and triphosgene (2.04 g, 6.87 mmol) in anhydrous CH_2Cl_2 (120 mL) under N_2 . The cooling bath was removed, and the reaction mixture was allowed to warm to room temperature over 5 min. *N*-BOC-protected hydroxylamine **8** (2.89 g, 21.7 mmol) was added followed by anhydrous pyridine (1.6 mL, $d = 0.978$ g/mL at 25 °C, 20 mmol) all at once at room temperature. The reaction mixture was stirred for 10 min at room temperature and was then filtered through a short silica plug. The plug was washed with CH_2Cl_2 and the filtrate was concentrated *in vacuo* to afford a yellow oil (5.85 g). The crude product was purified by column chromatography (silica gel/20:80 ethyl acetate-petroleum ether) to afford the title compound as a yellow oil (4.88 g, 79%). ^1H NMR (400 MHz, CDCl_3): δ 8.18 (dt, $J = 8.2, 0.7$ Hz, 1 H), 7.80 (s, 1 H), 7.73-7.66 (m, 2 H), 7.57-7.49 (m, 1 H), 5.73 (s, 2 H), 1.50 (s, 9 H). ^{13}C NMR (101 MHz, CDCl_3) δ 155.35, 155.29, 146.94, 134.24, 130.99, 129.17, 128.42, 125.26, 83.87, 67.67, 28.03. HRMS m/z (DART) calculated for MNH_4^+ 330.1296, found 330.1293.

5.2.10. *N*-(*t*-Butoxycarbonyl)-*N*-(2-nitrobenzyloxycarboxy)methanesulfonamide (**10**)

Methanesulfonyl chloride (0.253 mL, $d = 1.48$ g/mL at 25 °C,

3.27 mmol), DMAP (0.0390 g, 0.319 mmol) and triethylamine (0.447 mL, $d = 0.726$ g/mL at 25 °C, 3.21 mmol) were added to a stirred solution of **9** (1.00 g, 3.20 mmol) in anhydrous CH_2Cl_2 (35 mL) under N_2 at 0 °C - 2 °C. The mixture was stirred at 0 °C - 2 °C for 10 min and allowed to warm to room temperature with stirring until the reaction was complete (30 min). The mixture was passed through a base-treated (5% Et_3N) short silica plug and eluted using ethyl acetate followed by methanol. Concentration *in vacuo* gave a crude product (1.27 g) that was used in the next step without further purification, since the compound was unstable to silica column chromatography. Crude ^1H NMR (400 MHz, CDCl_3): δ 11.88 (s, 1 H), 8.21 (dd, $J = 8.2, 1.2$ Hz, 1 H), 7.81-7.64 (m, 2 H), 7.58-7.56 (m, 1 H), 5.79 (s, 2 H), 3.42 (s, 3 H), 1.56 (s, 9 H).

5.2.11. *N*-(2-Nitrobenzyloxycarboxy)methanesulfonamide (**1e**)

Trifluoroacetic acid (TFA, 4.000 mL, $d = 1.489$ g/mL at 20 °C, 52.24 mmol) was added all at once to a stirred solution of **10** (1.267 g, crude) in anhydrous CH_2Cl_2 (20 mL) under N_2 at room temperature. The mixture was stirred at room temperature, and the reaction was completed in 25 min. The solvent was removed *in vacuo*, and the TFA was removed by the successive addition and evaporation of CH_2Cl_2 (3×15 mL) to afford a yellow oil. The compound was then placed in a vacuum desiccator to remove the remaining solvent. A pale-yellow solid was obtained which was purified by column chromatography (silica gel/40:60 ethyl acetate-petroleum ether) to afford the title compound **1e** as an off-white solid (0.791 g, 85% over two steps). m.p. 118-121 °C. ^1H NMR (400 MHz, acetone- d_6) δ 9.96 (s, 1 H), 8.20 (dd, $J = 8.0, 1.1$ Hz, 1 H), 7.88-7.76 (m, 2 H), 7.73-7.66 (m, 1 H), 5.73 (s, 2 H), 3.18 (s, 3 H). ^{13}C NMR (101 MHz, acetone- d_6) δ 154.34, 135.05, 131.43, 130.60, 130.34, 125.94, 110.84, 68.45, 38.37. HRMS m/z (DART) calculated for MNH_4^+ 308.0547, found 308.0457.

5.2.12. *N*-benzyloxy-1,1,1-trifluoromethanesulfonamide (**19**)

Aqueous NaOH (50 mL, 5% w/w) was added to *O*-benzylhydroxylamine hydrochloride (4.067 g, 25.48 mmol) suspended in diethyl ether (75 mL) in one portion. After 0.5 h of vigorous stirring, the organic layer was separated, washed with brine (100 mL), and dried over MgSO_4 . The solution was filtered and concentrated *in vacuo* to give crude *O*-benzylhydroxylamine (2.981 g), which was subsequently used without further purification. To a solution of crude *O*-benzylhydroxylamine (2.981 g) dissolved in anhydrous CH_2Cl_2 (80 mL) was added anhydrous pyridine (1.96 mL, $d = 0.978$ g/mL at 25 °C, 24.2 mmol) and DMAP (2.958 g, 24.21 mmol). Trifluoromethanesulfonyl chloride (2.58 mL, $d = 1.583$ g/mL at 25 °C, 24.2 mmol) was added to the reaction mixture in one portion at -20 °C with cooling using a dry-ice ethanol bath. The reaction mixture was allowed to warm to room temperature over 0.5 h. After stirring for 4 h at room temperature, the reaction mixture was poured into saturated aqueous NaHCO_3 solution (100 mL). After layer separation, the organic layer was washed further with saturated CuSO_4 (50 mL). Then the organic layer was dried over MgSO_4 and concentrated *in vacuo*. The resulting crude solid was purified by column chromatography (silica gel/50:50 CH_2Cl_2 -petroleum ether) to give the title product **19** as a brown yellow solid (1.50 g, 23%). ^1H NMR (400 MHz, CDCl_3) δ 7.57 (s, 1 H), 7.43-7.36 (m, 5 H), 5.02 (s, 2 H). ^{19}F NMR (376 MHz, CDCl_3) δ -73.41.

5.3. General procedures for steady state photolysis

Photolysis experiments were carried out using a Rayonet mini-photoreactor (RMR-600) with 300 nm bulbs (4 W, 8 lamps). All photolysis samples were prepared in a mixture of phosphate buffer (pH 7.00, 0.10 M or 5.0 mM) and CD_3CN (40:60, v/v) in a sealed NMR tube fitted with a J-Young air-tight cap. 3-(Trimethylsilyl)propionic-2,2,3,3- d_4 acid sodium salt was used as an internal reference standard for ^1H NMR spectroscopy. Ph- CF_3 sealed in a capillary tube was used as an external reference standard for ^{19}F NMR spectroscopy. After each

irradiation, the sample was analyzed by ^1H and ^{19}F NMR spectroscopy.

5.4. Determining the molar extinction coefficient of **1a-d**

Standard solutions of **1a-1d** (150, 200, 250, 300, 350 and 400 μM) in a mixture of water and MeCN (92:8 v/v) were prepared and UV-Vis spectra were recorded (25.0 $^\circ\text{C}$). Molar extinction coefficients were obtained from plots of absorbance versus concentration, at 264 nm (**1a** and **1b**) or 351 nm (**1c** and **1d**).

6. Determination of the Photoproduct Quantum Yields of **1a-1e**

6.1. Control Experiment with Ferrioxalate

Prior to using *trans*-azobenzene to determine the quantum yield of compounds **1a-1e**, a control experiment was performed using another well-established actinometer, ferrioxalate. Potassium ferrioxalate was synthesized using a literature procedure [100]. The ratio of the quantum yields for ferrioxalate ($\Phi = 1.24$ in buffered acidic solution at 313 nm [101]) and *trans*-azobenzene ($\Phi = 0.14$ in MeOH at 313 nm [90]) was experimentally determined at 313 (± 3) nm, using a Xe lamp equipped with a monochromator (slit width 0.1 mm) using literature procedures [90]. The ratio of $\Phi(\text{azobenzene}):\Phi(\text{ferrioxalate})$ was 1: (0.13 \pm 0.01), which is in good agreement with the ratio calculated using literature values (1:0.11).

6.2. Photoproduct Quantum Yields of **1a-1e**

All experiments were carried out under aerobic conditions. Our control experiments demonstrate that both decomposition rate constants and photolytic products distribution from the photolysis of **1a-1e** obtained in the mixture of CD_3OD /phosphate buffer are the same in the absence or presence of air. A stock solution of compound **1a-e** (10.0 mM) in CD_3OD was used to prepare a series of solutions of **1a-e** (1.00 mM), with TSP and Ph- CF_3 as an internal reference for the ^1H and ^{19}F NMR experiments, respectively. For each compound the photolysis of a series of samples was carried out at 313 ± 3 nm (Xe lamp + monochromator), for a range of total irradiation times (± 3 s). After irradiation, an aliquot of each sample was transferred into an NMR tube and the photoproducts characterized by NMR spectroscopy (**1a** and **1c** : ^{19}F NMR; **1b**, **1d** and **1e** : ^1H NMR). The percentage decomposition of the starting material was less than 10% at the longest irradiation time. The moles of the photoproduct RSO_2NH_2 (R = Me or CF_3); determined from integration of a peak of the starting material and RSO_2NH_2 and the initial concentration of **1a-1d** prior to irradiation) and the total number of moles of the photoproduct MeSO_2NHOH and MeSO_3^- (determined from integration of a Me peak of the starting material, MeSO_2NHOH and MeSO_3^- and the initial concentration of **1e** prior to irradiation) was determined for each sample, and this value was plotted versus irradiation time (min). The slope of each plot of moles of photoproduct versus total irradiation time was determined (Fig. S9-S13).

A plot of moles of *cis*-azobenzene versus irradiation time was generated on the same day for the photoisomerisation of *trans*-azobenzene to *cis*-azobenzene using the identical experimental set up (Fig. S8). A solution of *trans*-azobenzene (6.60×10^{-5} M, $\epsilon_{313 \text{ nm}} = 22337 \text{ M}^{-1} \text{ cm}^{-1}$ [90]) in methanol was prepared and stored in the dark. An aliquot (3.00 mL) was transferred to a 10 mm quartz cuvette and the UV-vis spectrum was recorded. The aliquot was then irradiated for 0.66 min at 313 nm and the UV-vis spectrum again recorded. This was repeated for total irradiation times of 1.33, 2.00, 2.66, 3.33 and 4.00 min. The UV-vis spectrum was recorded after each irradiation. The conversion to *cis*-azobenzene did not exceed 8%. The number of moles of the product *cis*-azobenzene was calculated by using equation (1)

$$n_{\text{cis}} = \frac{A_{\text{trans}} - A_{\text{obs}}}{A_{\text{trans}} - A_{\text{cis}}} \times n_{\text{reactant}} \quad (1)$$

where n_{cis} is the number of moles of *cis*-azobenzene product, n_{reactant} is the number of moles of the *trans*-azobenzene reactant in the cuvette ($= 1.98 \times 10^{-7}$ mol), A_{trans} is the absorbance of *trans*-azobenzene reactant ($= 1.47$, $\epsilon_{313 \text{ nm}} = 22337 \text{ M}^{-1} \text{ cm}^{-1}$ for *trans*-azobenzene [90]), A_{cis} is the absorbance of *cis* azobenzene (0.147; $\epsilon_{313 \text{ nm}} = 2016 \text{ M}^{-1} \text{ cm}^{-1}$ for *cis*-azobenzene [102]) and A_{obs} is the observed absorbance at 313 nm.

The quantum yields (Φ) for compounds **1a-1e** were calculated using equation (2), with $\Phi(\text{trans-azobenzene}) = 0.14$ [90].

$$\varphi(\mathbf{1a-1e}) = \frac{\text{Slope}(\mathbf{1a-1e})/\text{Absorbance}(\mathbf{1a-1e})}{\text{Slope}(\text{azobenzene})/\text{Absorbance}(\text{azobenzene})} \times \varphi(\text{azobenzene}) \quad (2)$$

The absorbance of the solutions of **1a-1e** (1.00 mM) at the excitation wavelength were calculated using the molar extinction coefficient of each reactant at 313 nm ($\epsilon_{313 \text{ nm}} = (1.40 \pm 0.02) \times 10^3 \text{ M}^{-1} \text{ cm}^{-1}$, $(1.10 \pm 0.03) \times 10^3 \text{ M}^{-1} \text{ cm}^{-1}$, $(3.50 \pm 0.03) \times 10^3 \text{ M}^{-1} \text{ cm}^{-1}$, $(3.80 \pm 0.04) \times 10^3 \text{ M}^{-1} \text{ cm}^{-1}$ and $(1.35 \pm 0.04) \times 10^3 \text{ M}^{-1} \text{ cm}^{-1}$ for **1a-1e**, respectively).

Declaration of Competing Interest

The authors declare that they have no known competing financial interests or personal relationships that could have appeared to influence the work reported in this paper.

Acknowledgements

The authors gratefully acknowledge the U.S. National Science Foundation (CHE-1306644) and the Auckland University of Technology for support for this research. We also thank Dr. Mahinda Gangoda for assistance with NMR data collection, and Drs. Jacob T. Shelley, You Yi, and Dirk Friedrich for assistance with HRMS analyses.

Appendix A. Supplementary data

Supplementary material related to this article can be found, in the online version, at doi:<https://doi.org/10.1016/j.jphotochem.2019.112033>.

References

- [1] F. Doctorovich, P.J. Farmer, M.A. Marti, *The chemistry and biology of nitroxyl (HNO)*; Elsevier, Amsterdam, Netherlands, 2017.
- [2] J.M. Fukuto, A recent history of nitroxyl chemistry, pharmacology and therapeutic potential, *Br. J. Pharmacol.* 176 (2019) 135–146, <https://doi.org/10.1111/bph.14384>.
- [3] N. Paolucci, T. Katori, H.C. Champion, M.E. St. John, K.M. Miranda, J.M. Fukuto, D.A. Wink, D.A. Kass, Positive inotropic and lusitropic effects of HNO/NO- in failing hearts: Independence from β -adrenergic signaling, *Proc. Natl. Acad. Sci. U.S.A.* 100 (2003) 5537–5542, <https://doi.org/10.1073/pnas.0937302100>.
- [4] W.D. Gao, C.I. Murray, Y. Tian, X. Zhong, J.F. DuMond, X. Shen, B.A. Stanley, D.B. Foster, D.A. Wink, S.B. King, J.E. Van Eyk, N. Paolucci, Nitroxyl-mediated disulfide bond formation between cardiac myofilament cysteines enhances contractile function, *Circ. Res.* 111 (2012) 1002–1011, <https://doi.org/10.1161/circresaha.112.270827>.
- [5] H.N. Sabbah, C.G. Tocchetti, M. Wang, S. Daya, R.C. Gupta, R.S. Tunin, R. Mazhari, E. Takimoto, N. Paolucci, D. Cowart, W.S. Colucci, D.A. Kass, Nitroxyl (HNO): A novel approach for the acute treatment of heart failure, *Circ. Heart Fail.* 6 (2013) 1250–1258, <https://doi.org/10.1161/circheartfailure.113.000632>.
- [6] A. Arcaro, G. Lembo, C.G. Tocchetti, Nitroxyl (HNO) for treatment of acute heart failure, *Current Heart Failure Reports* 11 (2014) 227–235, <https://doi.org/10.1007/s11897-014-0210-z>.
- [7] M. Eberhardt, M. Dux, B. Namer, J. Miljkovic, N. Cordasic, C. Will, T.I. Kichko, J. de la Roche, M. Fischer, S.A. Suárez, D. Bikiel, K. Dorsch, A. Leffler, A. Babes, A. Lampert, J.K. Lennerz, J. Jacobi, M.A. Marti, F. Doctorovich, E.D. Högestätt, P.M. Zymunt, I. Ivanovic-Burmazovic, K. Messlinger, P. Reeh, M.R. Filipovic, H₂S and NO cooperatively regulate vascular tone by activating a neuroendocrine HNO-TRPA1-CGRP signalling pathway, *Nat. Commun.* 5 (2014), <https://doi.org/10.1038/ncomms5444>.

- 1038/ncomms5381 Article #4381.
- [8] B.K. Kemp-Harper, J.D. Horowitz, R.H. Ritchie, Therapeutic potential of nitroxyl (HNO) donors in the management of acute decompensated heart failure, *Drugs* 76 (2016) 1337–1348, <https://doi.org/10.1007/s40265-016-0631-y>.
- [9] C. Tita, E.M. Gilbert, A.B. Van Bakel, J. Grzybowski, G.J. Haas, M. Jarrah, S.H. Dunlap, S.S. Gottlieb, M. Klapholz, P.C. Patel, R. Pfister, T. Seidler, K.B. Shah, T. Zieliński, R.P. Venuti, D. Cowart, S.Y. Foo, A. Vishnevsky, V. Mitrovic, A Phase 2a dose-escalation study of the safety, tolerability, pharmacokinetics and haemodynamic effects of BMS-986231 in hospitalized patients with heart failure with reduced ejection fraction, *Eur. J. Heart Fail.* 19 (2017) 1321–1332, <https://doi.org/10.1002/ejhf.897>.
- [10] J.M. Fukuto, C.J. Cisneros, R.L. Kinkade, A comparison of the chemistry associated with the biological signaling and actions of nitroxyl (HNO) and nitric oxide (NO), *J. Inorg. Biochem.* 118 (2013) 201–208, <https://doi.org/10.1016/j.jinorgbio.2012.08.027>.
- [11] V. Shafirovich, S.V. Lyar, Nitroxyl and its anion in aqueous solutions: Spin states, protic equilibria, and reactivities toward oxygen and nitric oxide, *Proc. Natl. Acad. Sci. U.S.A.* 99 (2002) 7340–7345, <https://doi.org/10.1073/pnas.112202099>.
- [12] H. Nakagawa, Controlled release of HNO from chemical donors for biological applications, *J. Inorg. Biochem.* 118 (2013) 187–190, <https://doi.org/10.1016/j.jinorgbio.2012.10.004>.
- [13] K.M. Miranda, H.T. Nagasawa, J.P. Toscano, Donors of HNO, *Curr. Top. Med. Chem.* 5 (2005) 649–664, <https://doi.org/10.2174/1568026054679290>.
- [14] J.F. DuMond, S.B. King, The chemistry of nitroxyl-releasing compounds, *Antioxid. Redox Signal.* 14 (2011) 1637–1648, <https://doi.org/10.1089/ars.2010.3838>.
- [15] Z. Miao, S.B. King, Recent advances in the chemical biology of nitroxyl (HNO) detection and generation, *Nitric Oxide* 57 (2016) 1–14, <https://doi.org/10.1016/j.niox.2016.04.006>.
- [16] K. Sirsalmath, S.A. Suárez, D.E. Bikiel, F. Doctorovich, The pH of HNO donation is modulated by ring substituents in Pilot's acid derivatives: azanone donors at biological pH, *J. Inorg. Biochem.* 118 (2013) 134–139, <https://doi.org/10.1016/j.jinorgbio.2012.10.008>.
- [17] K. Aizawa, H. Nakagawa, K. Matsuo, K. Kawai, N. Ieda, T. Suzuki, N. Miyata, Pilot's acid derivative with improved nitroxyl-releasing characteristics, *Bioorg. Med. Chem. Lett.* 23 (2013) 2340–2343, <https://doi.org/10.1016/j.bmcl.2013.02.062>.
- [18] S.K. Adas, V. Bharadwaj, Y. Zhou, J. Zhang, A.J. Seed, N.E. Brasch, P. Sampson, Synthesis and HNO donating properties of the Pilot's acid analogue trifluoromethanesulfonylhydroxamic acid: Evidence for quantitative release of HNO at neutral pH conditions, *Chem.-Eur. J.* 24 (2018) 7330–7334, <https://doi.org/10.1002/chem.201800662>.
- [19] D.A. Guthrie, N.Y. Kim, M.A. Siegler, C.D. Moore, J.P. Toscano, Development of *N*-substituted hydroxylamines as efficient nitroxyl (HNO) donors, *J. Am. Chem. Soc.* 134 (2012) 1962–1965, <https://doi.org/10.1021/ja2103923>.
- [20] A.D. Sutton, M. Williamson, H. Weismiller, J.P. Toscano, Optimization of HNO production from *N,O*-bis-acylated hydroxylamine derivatives, *Org. Lett.* 14 (2012) 472–475, <https://doi.org/10.1021/ol203016c>.
- [21] D.A. Guthrie, A. Ho, C.G. Takahashi, A. Collins, M. Morris, J.P. Toscano, Catch-and-release" of HNO with pyrazolones, *J. Org. Chem.* 80 (2015) 1338–1348, <https://doi.org/10.1021/jo502330w>.
- [22] D.A. Guthrie, S. Nourian, C.G. Takahashi, J.P. Toscano, Curtailing the hydroxylaminobarbituric acid-hydantoin rearrangement to favor HNO generation, *J. Org. Chem.* 80 (2015) 1349–1356, <https://doi.org/10.1021/jo5023316>.
- [23] S. Nourian, R.P. Lesko, D.A. Guthrie, J.P. Toscano, Nitrosocarbonyl release from *O*-substituted hydroxamic acids with pyrazolone leaving groups, *Tetrahedron* 72 (2016) 6037–6042, <https://doi.org/10.1016/j.tet.2016.08.016>.
- [24] S. Nourian, Z.A. Zilber, J.P. Toscano, Development of *N*-substituted hydroxamic acids with pyrazolone leaving groups as nitrosocarbonyl precursors, *J. Org. Chem.* 81 (2016) 9138–9146, <https://doi.org/10.1021/acs.joc.6b01705>.
- [25] D. Andrei, D.J. Salmon, S. Donzelli, A. Wahab, J.R. Klose, M.L. Citro, J.E. Saavedra, D.A. Wink, K.M. Miranda, L.K. Keefer, Dual mechanisms of HNO generation by a nitroxyl prodrug of the diazeniumdiolate (NONOate) class, *J. Am. Chem. Soc.* 132 (2010) 16526–16532, <https://doi.org/10.1021/ja106552p>.
- [26] D.J. Salmon, C.L. Torres de Holding, L. Thomas, K.V. Peterson, G.P. Goodman, J.E. Saavedra, A. Srinivasan, K.M. Davies, L.K. Keefer, K.M. Miranda, HNO and NO release from a primary amine-based diazeniumdiolate as a function of pH, *Inorg. Chem.* 50 (2011) 3262–3270, <https://doi.org/10.1021/ic101736e>.
- [27] G. Bharadwaj, P.G.Z. Benini, D. Basudhar, C.N. Ramos-Colon, G.M. Johnson, M.M. Lariva, L.K. Keefer, D. Andrei, K.M. Miranda, Analysis of the HNO and NO donating properties of alicyclic amine diazeniumdiolates, *Nitric Oxide* 42 (2014) 70–78, <https://doi.org/10.1016/j.niox.2014.08.013>.
- [28] X. Sha, T.S. Isbell, R.P. Patel, C.S. Day, S.B. King, Hydrolysis of acyloxy nitroso compounds yields nitroxyl (HNO), *J. Am. Chem. Soc.* 128 (2006) 9687–9692, <https://doi.org/10.1021/ja062365a>.
- [29] J.F. DuMond, M.W. Wright, S.B. King, Water soluble acyloxy nitroso compounds: HNO release and reactions with heme and thiol containing proteins, *J. Inorg. Biochem.* 118 (2013) 140–147, <https://doi.org/10.1016/j.jinorgbio.2012.07.023>.
- [30] S. Mitroka, M.E. Shoman, J.F. DuMond, L. Bellavia, O.M. Aly, M. Abdel-Aziz, D.B. Kim-Shapiro, S.B. King, Direct and nitroxyl (HNO)-mediated actions of acyloxy nitroso compounds with the thiol-containing proteins glyceraldehyde 3-phosphate dehydrogenase and alkyl hydroperoxide reductase subunit C, *J. Med. Chem.* 56 (2013) 6583–6592, <https://doi.org/10.1021/jm400057r>.
- [31] H.A.H. Mohamed, M. Abdel-Aziz, G.E.A.A. Abuo-Rahma, S.B. King, New acyloxy nitroso compounds with improved water solubility and nitroxyl (HNO) release kinetics and inhibitors of platelet aggregation, *Bioorg. Med. Chem.* 23 (2015) 6069–6077, <https://doi.org/10.1016/j.bmc.2015.04.023>.
- [32] R.N. Atkinson, B.M. Storey, S.B. King, Reactions of acyl nitroso compounds with amines: Production of nitroxyl (HNO) with the preparation of amides, *Tetrahedron Lett.* 37 (1996) 9287–9290, [https://doi.org/10.1016/s0040-4039\(97\)82943-7](https://doi.org/10.1016/s0040-4039(97)82943-7).
- [33] A.D. Cohen, B.-B. Zeng, S.B. King, J.P. Toscano, Direct observation of an acyl nitroso species in solution by time-resolved IR spectroscopy, *J. Am. Chem. Soc.* 125 (2003) 1444–1445, <https://doi.org/10.1021/ja028978e>.
- [34] Y. Adachi, H. Nakagawa, K. Matsuo, T. Suzuki, N. Miyata, Photoactivatable HNO-releasing compounds using the retro-Diels-Alder reaction, *Chem. Commun.* (2008) 5149–5151, <https://doi.org/10.1039/b811985f>.
- [35] K. Matsuo, H. Nakagawa, Y. Adachi, H. Kameda, H. Tsumoto, T. Suzuki, N. Miyata, Alternative photoinduced release of HNO or NO from an acyl nitroso compound, depending on environmental polarity, *Chem. Commun.* 46 (2010) 3788–3790, <https://doi.org/10.1039/c001502d>.
- [36] A.S. Evans, A.D. Cohen, Z.A. Gurard-Levin, N. Kebede, T.C. Celius, A.P. Miceli, J.P. Toscano, Photogeneration and reactivity of acyl nitroso compounds, *Can. J. Chem.* 89 (2011) 130–138, <https://doi.org/10.1139/v10-10-11>.
- [37] M.G. Memeo, D. Dondi, B. Mannucci, F. Corana, P. Quadrelli, HNO made-easy from photochemical cycloreversion of novel 3,5-heterocyclic disubstituted 1,2,4-oxadiazole-4-oxides, *Tetrahedron* 69 (2013) 7387–7394, <https://doi.org/10.1016/j.tet.2013.06.067>.
- [38] K.P. Schultz, D.W. Spivey, E.K. Loya, J.E. Kellon, L.M. Taylor, M.R. McConville, Photochemical locking and unlocking of an acyl nitroso dienophile in the Diels-Alder reaction, *Tetrahedron Lett.* 57 (2016) 1296–1299, <https://doi.org/10.1016/j.tetlet.2016.02.044>.
- [39] B.-B. Zeng, J. Huang, M.W. Wright, S.B. King, Nitroxyl (HNO) release from new functionalized *N*-hydroxyurea-derived acyl nitroso-9,10-dimethylanthracene cycloadducts, *Bioorg. Med. Chem. Lett.* 14 (2004) 5565–5568, <https://doi.org/10.1016/j.bmcl.2004.08.062>.
- [40] C.H. Switzer, T.W. Miller, P.J. Farmer, J.M. Fukuto, Synthesis and characterization of lithium oxonitrate (LiNO), *J. Inorg. Biochem.* 118 (2013) 128–133, <https://doi.org/10.1016/j.jinorgbio.2012.09.022>.
- [41] M.A. Rhine, A.V. Rodrigues, R.J.B. Urbauer, J.L. Urbauer, T.L. Stemmler, T.C. Harrop, Proton-induced reactivity of NO⁻ from a {CoNO}⁸ complex, *J. Am. Chem. Soc.* 136 (2014) 12560–12563, <https://doi.org/10.1021/ja506444a>.
- [42] Y.-T. Tseng, C.-H. Chen, J.-Y. Lin, B.-H. Li, Y.-H. Lu, C.-H. Lin, H.-T. Chen, T.-C. Weng, D. Sokaras, H.-Y. Chen, Y.-L. Soo, T.-T. Lu, To transfer or not to transfer? Development of a dinitrosyl iron complex as a nitroxyl donor for the nitroxylation of an Fe-III-porphyrin center, *Chem.-Eur. J.* 21 (2015) 17570–17573, <https://doi.org/10.1002/chem.201503176>.
- [43] M.R. Walter, S.P. Dzul, A.V. Rodrigues, T.L. Stemmler, J. Telsler, J. Conradie, A. Ghosh, T.C. Harrop, Synthesis of Co^{II}-NO⁻ complexes and their reactivity as a source of nitroxyl, *J. Am. Chem. Soc.* 138 (2016) 12459–12471, <https://doi.org/10.1021/jacs.6b05896>.
- [44] F.T. Bonner, Y. Ko, Kinetic, isotopic, and ¹⁵N NMR study of *N*-hydroxybenzenesulfonamide decomposition: An HNO source reaction, *Inorg. Chem.* 31 (1992) 2514–2519, <https://doi.org/10.1021/ic00038a038>.
- [45] G. Carrone, J. Pellegrino, F. Doctorovich, Rapid generation of HNO induced by visible light, *Chem. Commun.* 53 (2017) 5314–5317, <https://doi.org/10.1039/c7cc02186k>.
- [46] Y. Zhou, R.B. Cink, R.S. Dassanayake, A.J. Seed, N.E. Brasch, P. Sampson, Rapid photoactivated generation of nitroxyl (HNO) under neutral pH conditions, *Angew. Chem., Int. Ed.* 55 (2016) 13229–13232, <https://doi.org/10.1002/anie.201605160>.
- [47] Y. Zhou, R.B. Cink, Z.A. Fejedelem, M.C. Simpson, A.J. Seed, P. Sampson, N.E. Brasch, Development of photoactivatable nitroxyl (HNO) donors incorporating the (3-hydroxy-2-naphthalenyl)methyl phototrigger, *Eur. J. Org. Chem.* (2018) 1745–1755, <https://doi.org/10.1002/ejoc.201800092>.
- [48] M. Kawaguchi, T. Tani, R. Hombu, N. Ieda, H. Nakagawa, Development and cellular application of visible-light-controllable HNO releasers based on caged Pilot's acid, *Chem. Commun.* 54 (2018) 10371–10374, <https://doi.org/10.1039/c8cc04954h>.
- [49] Y. Zhou, R.B. Cink, A.J. Seed, M.C. Simpson, P. Sampson, N.E. Brasch, Stoichiometric nitroxyl photorelease using the (6-hydroxy-2-naphthalenyl)methyl phototrigger, *Org. Lett.* 21 (2019) 1054–1057, <https://doi.org/10.1021/acs.orglett.8b04099>.
- [50] P. Wang, Photolabile protecting groups: Structure and reactivity, *Asian J. Org. Chem.* 2 (2013) 452–464, <https://doi.org/10.1002/ajoc.201200197>.
- [51] P. Klán, T. Šolomek, C.G. Bochet, A. Blanc, R. Givens, M. Rubina, V. Popik, A. Kostikov, J. Wirz, Photoremovable protecting groups in chemistry and biology: Reaction mechanisms and efficacy, *Chem. Rev.* 113 (2013) 119–191, <https://doi.org/10.1021/cr300177k>.
- [52] A. Hasan, K.-P. Stengele, H. Giegrich, P. Cornwell, K.R. Isham, R.A. Sachleben, W. Pfeleiderer, R.S. Foote, Photolabile protecting groups for nucleosides: Synthesis and photodeprotection rates, *Tetrahedron* 53 (1997) 4247–4264, [https://doi.org/10.1016/s0040-4020\(97\)00154-3](https://doi.org/10.1016/s0040-4020(97)00154-3).
- [53] H. Yu, J. Li, D. Wu, Z. Qiu, Y. Zhang, Chemistry and biological applications of photo-labile organic molecules, *Chem. Soc. Rev.* 39 (2010) 464–473, <https://doi.org/10.1039/b901255a>.
- [54] E. Riguet, C.G. Bochet, New safety-catch photolabile protecting group, *Org. Lett.* 9 (2007) 5453–5456, <https://doi.org/10.1021/ol702327c>.
- [55] R.J.T. Mikkelsen, K.E. Grier, K.T. Mortensen, T.E. Nielsen, K. Qvortrup, Photolabile linkers for solid-phase synthesis, *ACS Comb. Sci.* 20 (2018) 377–399, <https://doi.org/10.1021/acscombsci.8b00028>.
- [56] I. Aujard, C. Benbrahim, M. Gouget, O. Ruel, J.-B. Baudin, P. Neveu, L. Jullien, o-Nitrobenzyl photolabile protecting groups with red-shifted absorption: Syntheses and uncaging cross-sections for one- and two-photon excitation, *Chem.-Eur. J.* 12

- (2006) 6865–6879, <https://doi.org/10.1002/chem.200501393>.
- [57] Y.V. Il'ichev, M.A. Schwörer, J. Wirz, Photochemical reaction mechanisms of 2-nitrobenzyl compounds: Methyl ethers and caged ATP, *J. Am. Chem. Soc.* 126 (2004) 4581–4595, <https://doi.org/10.1021/ja039071z>.
- [58] D.D. Young, A. Deiters, Photochemical control of biological processes, *Org. Biomol. Chem.* 5 (2007) 999–1005, <https://doi.org/10.1039/b616410m>.
- [59] K.A. Ryu, L. Stutts, J.K. Tom, R.J. Mancini, A.P. Esser-Kahn, Stimulation of innate immune cells by light-activated TLR7/8 agonists, *J. Am. Chem. Soc.* 136 (2014) 10823–10825, <https://doi.org/10.1021/ja412314j>.
- [60] V. Grenier, A.S. Walker, E.W. Miller, A small-molecule photoactivatable optical sensor of transmembrane potential, *J. Am. Chem. Soc.* 137 (2015) 10894–10897, <https://doi.org/10.1021/jacs.5b05538>.
- [61] R. Horbert, B. Pinchuk, P. Davies, D. Alessi, C. Peifer, Photoactivatable prodrugs of antimelanoma agent vemurafenib, *ACS Chem. Biol.* 10 (2015) 2099–2107, <https://doi.org/10.1021/acscchembio.5b00174>.
- [62] C. Bao, L. Zhu, Q. Lin, H. Tian, Building biomedical materials using photochemical bond cleavage, *Adv. Mater.* 27 (2015) 1647–1662, <https://doi.org/10.1002/adma.201403783>.
- [63] J. Kohl-Landgraf, F. Buhr, D. Lefrancquois, J.-M. Mewes, H. Schwalbe, A. Dreuw, J. Wachtveitl, Mechanism of the photoinduced uncaging reaction of puromycin protected by a 6-nitroveratryloxycarbonyl group, *J. Am. Chem. Soc.* 136 (2014) 3430–3438, <https://doi.org/10.1021/ja410594y>.
- [64] S. Wexler, H. Schayek, K. Rajendar, I. Tal, E. Shani, Y. Meroz, R. Dobrovetsky, R. Weinstain, Characterizing gibberellin flow *in planta* using photocaged gibberellins, *Chem. Sci.* 10 (2019) 1500–1505, <https://doi.org/10.1039/c8sc04528c>.
- [65] T. Schneider, J. Martin, P.M. Durkin, V. Kubyskhin, N. Budisa, The regioselective synthesis of *o*-nitrobenzyl DOPA derivatives, *Synthesis* 49 (2017) 2691–2699, <https://doi.org/10.1055/s-0036-1588766>.
- [66] Y. Zhao, S.G. Bolton, M.D. Pluth, Light-activated COS/H₂S donation from photocaged thiocarbamates, *Org. Lett.* 19 (2017) 2278–2281, <https://doi.org/10.1021/acs.orglett.7b00808>.
- [67] W. Liu, L. Liang, L. Zhao, H. Tan, J. Wu, Q. Qin, X. Gou, X. Sun, Synthesis and characterization of a photoresponsive doxorubicin/combretastatin A4 hybrid prodrug, *Bioorg. Med. Chem. Lett.* 29 (2019) 487–490, <https://doi.org/10.1016/j.bmcl.2018.12.017>.
- [68] S. Serra, A. Alouane, T. Le Saux, S. Huvelle, R. Plasson, F. Schmidt, L. Jullien, R. Labrère, A chemically encoded timer for dual molecular delivery at tailored rates and concentrations, *Chem. Commun.* 54 (2018) 6396–6399, <https://doi.org/10.1039/c8cc03253j>.
- [69] C. Mu, M. Shi, P. Liu, L. Chen, G. Marriotti, Daylight-mediated, passive, and sustained release of the glaucoma drug timolol from a contact lens, *ACS Central Sci.* 4 (2018) 1677–1687, <https://doi.org/10.1021/acscentsci.8b00641>.
- [70] H. Yan, U. Bhattarai, Y. Song, F.-S. Liang, Design, synthesis and activity of light deactivatable microRNA inhibitor, *Bioorganic Chem.* 80 (2018) 492–497, <https://doi.org/10.1016/j.bioorg.2018.07.003>.
- [71] B. Pinchuk, R. Horbert, A. Döbber, L. Kuhl, C. Peifer, Photoactivatable caged prodrugs of VEGFR-2 kinase inhibitors, *Molecules* 21 (2016) 570, <https://doi.org/10.3390/molecules21050570>.
- [72] M.A. Romero, N. Basilio, A.J. Moro, M. Domingues, J.A. González-Delgado, J.F. Arteaga, U. Pischel, Photocaged competitor guests: A general approach toward light-activated cargo release from cucurbiturils, *Chem.-Eur. J.* 23 (2017) 13105–13111, <https://doi.org/10.1002/chem.201702185>.
- [73] A. Döbber, A.F. Phoa, R.H. Abbassi, B.W. Stringer, B.W. Day, T.G. Johns, M. Abadie, C. Peifer, L. Munoz, Development and biological evaluation of a photoactivatable small molecule microtubule-targeting agent, *ACS Med. Chem. Lett.* 8 (2017) 395–400, <https://doi.org/10.1021/acsmchemlett.6b00483>.
- [74] W. Zhang, F. Hamouri, Z. Feng, I. Atujard, B. Ducos, S. Ye, S. Weiss, M. Volovitch, S. Vriz, L. Jullien, D. Bensimon, Control of protein activity and gene expression by cyclofen-OH uncaging, *ChemBioChem* 19 (2018) 1232–1238, <https://doi.org/10.1002/cbic.201700630>.
- [75] W.R. Grither, J. Korang, J.P. Sauer, M.P. Sherman, P.L. Vanegas, M. Zhang, R.D. McCulla, The effect of nitro substitution on the photochemistry of benzyl benzoxyhydroxamate: Photoinduced release of benzoxyhydroxamic acid, *J. Photochem. Photobiol., A* 227 (2012) 1–10, <https://doi.org/10.1016/j.jphotochem.2011.10.005>.
- [76] A. Leonidova, C. Mari, C. Aebersold, G. Gasser, Selective photorelease of an organometallic-containing enzyme inhibitor, *Organometallics* 35 (2016) 851–854, <https://doi.org/10.1021/acs.organomet.6b00029>.
- [77] B. Parasar, P.V. Chang, Chemical optogenetic modulation of inflammation and immunity, *Chem. Sci.* 8 (2017) 1450–1453, <https://doi.org/10.1039/c6sc03702j>.
- [78] I. Seven, T. Weinrich, M. Gränz, C. Grünewald, S. Brüß, I. Krstić, T.F. Prisner, A. Heckel, M.W. Göbel, Photolabile protecting groups for nitroxide spin labels, *Eur. J. Org. Chem.* (2014) 4037–4043, <https://doi.org/10.1002/ejoc.201301692>.
- [79] C.D. McCune, S.J. Chan, M.L. Beio, W.J. Shen, W. Chung, L.M. Szczesniak, C. Chai, S.Q. Koh, P.T.-H. Wong, D.B. Berkowitz, "Zipped synthesis" by cross-metathesis provides a cystathionine β-synthase inhibitor that attenuates cellular H2S levels and reduces neuronal infarction in a rat ischemic stroke model, *ACS Cent. Sci.* 2 (2016) 242–252, <https://doi.org/10.1021/acscentsci.6b00019>.
- [80] K. Qvortrup, T.E. Nielsen, In-bead screening of hydroxamic acids for the identification of HDAC inhibitors, *Angew. Chem., Int. Ed.* 55 (2016) 4472–4475, <https://doi.org/10.1002/anie.201511308>.
- [81] K. Qvortrup, R.G. Petersen, A.O. Dohn, K.B. Møller, T.E. Nielsen, Solvent-controlled chemoselectivity in the photolytic release of hydroxamic acids and carboxamides from solid support, *Org. Lett.* 19 (2017) 3263–3266, <https://doi.org/10.1021/acs.orglett.7b01386>.
- [82] J. Olejniczak, M. Chan, A. Almutairi, Light-triggered intramolecular cyclization in poly(lactic-co-glycolic acid)-based polymers for controlled degradation, *Macromolecules* 48 (2015) 3166–3172, <https://doi.org/10.1021/acs.macromol.5b00455>.
- [83] P.J. Bunyan, J.I.G. Cadogan, The reactivity of organophosphorus compounds. Part XIV. Deoxygenation of aromatic C-nitroso-compounds by triethyl phosphite and triphenylphosphine: A new cyclisation reaction, *J. Chem. Soc.* (1963) 42–49, <https://doi.org/10.1039/jr9630000042>.
- [84] J.I.G. Cadogan, Reduction of nitro- and nitroso-compounds by trivalent phosphorus reagents, *Quart. Rev.* 22 (1968) 222–251, <https://doi.org/10.1039/qr9682200222>.
- [85] S. Kuberski, J. Gębicki, Evidence for a ketene intermediate in the photochemical transformation of matrix-isolated *o*-nitrobenzaldehyde, *J. Mol. Struct.* 275 (1992) 105–110, [https://doi.org/10.1016/0022-2860\(92\)80185-k](https://doi.org/10.1016/0022-2860(92)80185-k).
- [86] J. Choi, M. Terazima, Photochemical reaction of 2-nitrobenzaldehyde by monitoring the diffusion coefficient, *J. Phys. Chem. B* 107 (2003) 9552–9557, <https://doi.org/10.1021/jp0342071>.
- [87] D. Gerbig, P.R. Schreiner, Formation of a tunneling product in the photorearrangement of *o*-nitrobenzaldehyde, *Angew. Chem., Int. Ed.* 56 (2017) 9445–9448, <https://doi.org/10.1002/anie.201705140>.
- [88] M.V. George, J.C. Scaiano, Photochemistry of *o*-nitrobenzaldehyde and related studies, *J. Phys. Chem.* 84 (1980) 492–495, <https://doi.org/10.1021/j100442a007>.
- [89] S. Laingruber, W.J. Schreier, T. Schrader, F. Koller, W. Zinth, P. Gilch, The photochemistry of *o*-nitrobenzaldehyde as seen by femtosecond vibrational spectroscopy, *Angew. Chem., Int. Ed.* 44 (2005) 7901–7904, <https://doi.org/10.1002/anie.200501642>.
- [90] V. Ladányi, P. Dvořák, J. Al Anshori, L. Vetráková, J. Wirz, D. Heger, Azobenzene photoisomerization quantum yields in methanol redetermined, *Photochem. Photobiol. Sci.* 16 (2017) 1757–1761, <https://doi.org/10.1039/c7pp00315c>.
- [91] T. Šolomek, S. Mercier, T. Bally, C.G. Bochet, Photolysis of *ortho*-nitrobenzyl derivatives: the importance of the leaving group, *Photochem. Photobiol. Sci.* 11 (2012) 548–555, <https://doi.org/10.1039/c1pp05308f>.
- [92] T. Šolomek, C.G. Bochet, T. Bally, The primary steps in excited-state hydrogen transfer: The phototautomerization of *o*-nitrobenzyl derivatives, *Chem.-Eur. J.* 20 (2014) 8062–8067, <https://doi.org/10.1002/chem.201303338>.
- [93] J.E.T. Corrie, A. Barth, V.R.N. Munasinghe, D.R. Trentham, M.C. Hutter, Photolytic cleavage of 1-(2-nitrophenyl)ethyl ethers involves two parallel pathways and product release is rate-limited by decomposition of a common hemiacetal intermediate, *J. Am. Chem. Soc.* 125 (2003) 8546–8554, <https://doi.org/10.1021/ja034354c>.
- [94] M. Schwörer, J. Wirz, Photochemical reaction mechanisms of 2-nitrobenzyl compounds in solution I. 2-nitrotoluene: Thermodynamic and kinetic parameters of the *aci*-nitro tautomer, *Helv. Chim. Acta* 84 (2001) 1441–1458, [10.1002/1522-2675\(20010613\)84:6<1441::Aid-hlca1441>3.0.Co;2-w](https://doi.org/10.1002/1522-2675(20010613)84:6<1441::Aid-hlca1441>3.0.Co;2-w).
- [95] E. Lipczynska-Kochany, Photochemistry of hydroxamic acids and derivatives, *Chem. Rev.* 91 (1991) 477–491, <https://doi.org/10.1021/cr00004a002>.
- [96] J.E. Johnson, M. Arfan, R. Hodzi, L.R. Caswell, S. Rasmussen, Mechanisms of photoelimination reactions of alkyl benzoxyhydroxamates, *Photochem. Photobiol.* 51 (1990) 139–144, <https://doi.org/10.1111/j.1751-1097.1990.tb01694.x>.
- [97] R.D. Trepka, J.K. Harrington, J.W. Belisle, Acidities and partition coefficients of fluoromethanesulfonamides, *J. Org. Chem.* 39 (1974) 1094–1098, <https://doi.org/10.1021/jo00922a017>.
- [98] F.G. Bordwell, Equilibrium acidities in dimethyl sulfoxide solution, *Acc. Chem. Res.* 21 (1988) 456–463, <https://doi.org/10.1021/ar00156a004>.
- [99] G.E.K. Branch, J.O. Clayton, The strength of acetamide as an acid, *J. Am. Chem. Soc.* 50 (1928) 1680–1686, <https://doi.org/10.1021/ja01393a023>.
- [100] J. Olmsted III, Preparation and analysis of potassium tris(oxalato)ferrate(III) trihydrate - a general-chemistry experiment, *J. Chem. Educ.* 61 (1984) 1098–1099, <https://doi.org/10.1021/ed061p1098>.
- [101] J. Lee, H.H. Seliger, Quantum yield of the ferrioxalate actinometer, *J. Chem. Phys.* 40 (1964) 519–523, <https://doi.org/10.1063/1.1725147>.
- [102] L. Vetráková, V. Ladányi, J. Al Anshori, P. Dvořák, J. Wirz, D. Heger, The absorption spectrum of *cis*-azobenzene, *Photochem. Photobiol. Sci.* 16 (2017) 1749–1756, <https://doi.org/10.1039/c7pp00314e>.